Studsvik

Document #: SSP-14/P01-028-TR-NP
Revision #: 0

Generic Application of the Studsvik Scandpower Core Management System to Pressurized Water Reactors

December, 2015

Prepared by: Digitally signed by Brandon Haugh
Date: 2015.12.17 14:20:11 -05'00'

Brandon P. Haugh, Senior Engineer Date

Reviewed by: Joel Rhodes III Digitally signed by Joel Rhodes III
Date: 2015.12.17 12:34:38 -07'00'

Joel D. Rhodes, III, Methods Manager Date

Approved by: David Kropaczek
2015.12.18 15:55:48 -05'00'

Dave Kropaczek, President Date

Proprietary Statement

This report is proprietary to Studsvik Scandpower, Inc. (SSP). The recipient company and/or any of its employees shall not reproduce copy, publish or otherwise disclose this report or the SSP information therein to any third party without written permission from Studsvik Scandpower, Inc.

This report contains information proprietary to Studsvik Scandpower, Inc. (SSP). A nonproprietary version of this report has also been prepared for distribution to the United States Nuclear Regulatory Commission (NRC). To conform to the requirements of the Commission's regulations (10CFR2.390) concerning the protection of proprietary information submitted to the NRC, the proprietary information in the proprietary version of this document is contained within brackets {}; where the proprietary information has been deleted in the nonproprietary versions, only the brackets remain (to indicate that the information contained within the brackets in the proprietary versions has been deleted). Pursuant to 10CFR2.390(b)(1), justification for claiming the information being so designated is provided in the affidavit accompanying the transmittal of these documents.

Copyright Notice

Abstract

As part of Studsvik Scandpower Inc's commitment to providing our customers with the most modern production core analysis tools, the CMS5 system of codes has been applied generically to the modeling and analysis of PWR cores. The CMS5 code system consists of CASMO5, CMSLINK5 and SIMULATE5. The accuracy of the CMS5 code system is demonstrated through an extensive set of benchmarks including validation to critical experiments and higher-order codes and a 7 unit / 63 cycle comparison of predictions to PWR plant data. A rigorous methodology is presented to calculate Nuclear Uncertainty Factors for physics parameters for which CMS5 predictions can be compared against measurements or higher-order codes. Based on the extensive nature of the 63 cycle benchmark that includes a wide array of PWR design and operating data, a set of conservative generic Nuclear Reliability Factors were determined to account for model predictive bias and uncertainty.

Revision History

Revision Number	Description	Date
0	Original Documents	December, 2015

Table of Contents

Table of Figures

Table of Tables

1. Introduction

1.1 Background

The Studsvik Scandpower Core Management System (CMS) consists primarily of:

1. The CASMO two dimensional lattice physics code
2. The SIMULATE three dimensional analytical nodal code for the steady state analysis of both PWRs and BWRs.

The CMS package is used and accepted in the nuclear industry both in the United States and worldwide. The most widely adopted major versions of the codes in use today are CASMO-3 / CASMO-4 and SIMULATE-3, which have been used in reload physics design applications for nearly 25 years.

Nuclear power plant license holders have individually submitted requests to use the CMS system for core reload design, core follow, calculation of key core parameters for reload safety analysis, and related physics applications. Examples of such submittals are in References [1-4].

The CMS5 system (CASMO5 & SIMULATE5) is the latest generation of physics software that includes significant modeling enhancements that are described in Section 2.

1.2 Purpose

The purpose of this report is to present the CMS5 software system, an associated uncertainty factor methodology, and a generic set of core physics parameter uncertainty factors for generic approval for PWR core physics applications.

1.3 Organization

Section 2 of this report provides a description of the CMS5 software system and a validation of the software using comparisons to critical experiments and higher order codes. Section 3 of this report is a presentation of the methodology to produce uncertainty factors that are applied to CMS5 predictions for use in reload physics applications. Section 4 of this report provides a 7 unit / 63 cycle PWR benchmark of the CMS5 system, details a worked demonstration of the uncertainty factor methodology, and presents a set of generic reliability factors for PWR applications for review and approval.

Each section or sub-section of this report has a self-contained references section.

1.4 Adoption

It is expected that the main adoption mechanism of this generic methodology will be through the process described in U.S. N.R.C. Generic Letter 83-11, Supplement 1 (Reference [5]). Studsvik has the capability to provide assistance to licensees in meeting the procedural, training, comparison calculation, quality assurance and change control requirements of G.L. 83-11.

At the time a licensee sends the required notification to the NRC that it has followed the guidelines of G.L. 83-11 and intends to use the methodology described in this report for licensing applications, the licensee shall also notify the NRC of the set of Nuclear Reliability Factors (NRFs) it intends to use for those applications. This is an additional requirement relative to G.L. 83-11 in recognition of the capability granted by this methodology for licensees to either generate their own Nuclear Uncertainty Factors or to adopt the generic NRFs described in Section 4.6.

1.5 References

1. R. A. Hall et al., Dominion, “Qualification of the Studsvik Core Management System Reactor Physics Methods for Application to North Anna and Surry Power Stations”, DOM-NAF-1-Rev 0.0-P-A, NRC Safety Evaluation Date: March 2003, **NRC Accession Number: ML031690108**
2. Duke Energy Carolinas, “Oconee Nuclear Design Methodology Using CASMO-4 / SIMULATE-3”, DPC-NE-1006-A, Revision 0a, NRC Safety Evaluation Date: August 2011, **NRC Accession Number: ML101580106**
3. S.G. Zimmerman et al., Arizona Public Service Company, “PWR Reactor Physics Methodology Using CASMO-4/SIMULATE-3”, Enclosure 3 to Reference [4], **NRC Accession Number: ML010440094**
4. Arizona Public Service Company, “Palo Verde Nuclear Generating Station (PVNGS) Units 1,2 and 3 – Request for Amendment to Technical Specification 5.6.5, Core Operating Limits Report (COLR) (CASMO-4/SIMULATE-3)”, Letter dated June, 2000, **NRC Accession Number: ML003723799**
5. United States Nuclear Regulatory Commission, Generic Letter 83-11, Supplement 1, “Licensee Qualification for Performing Safety Analyses”, June 24, 1999

2. CMS5 Design and Validation

2.1 Introduction

2.1.1 Purpose

The purpose of this section is to present a high level description of the CMS5 code system as applied to Pressurized Water Reactors (PWRs). Following the software descriptions an overview is given of the validation and benchmarking performed in support of the Topical Report with the objective of demonstrating that the codes are robust and accurate.

2.2 Software Description

The Core Management System (CMS) codes are used to perform the neutronic and thermal hydraulic analysis needed for the design, optimization, and safety analysis of nuclear reactor cores. The system comprises three computer codes: CASMO5, CMSLINK5 and SIMULATE5.

These codes represent the state of the art for modern production methods for analyzing light water reactor cores. The CMS5 system builds on the decades of experience from CASMO3/4 and SIMULATE-3 while improving both the robustness and modeling details within the codes.

The following subsections present a short description of the key attributes and methods of each code along with supporting references where more detail is required.

2.2.1 CASMO5

CASMO5 [1] is a multigroup two-dimensional transport theory code for burnup calculations on PWR assemblies or simple pin cells. The code handles a geometry consisting of cylindrical fuel rods of varying composition in a square pitch array with allowance for absorber-loaded fuel rods, Integral Fuel Burnable Absorber (IFBA), burnable absorber rods, cluster control rods, in-core instrument channels, and water gaps. Reflector and baffle calculations can also be performed with CASMO5.

CASMO5 incorporates the direct microscopic depletion of burnable absorbers into the main calculation and a fully heterogeneous model is used for the two-dimensional transport calculation.

Some characteristics of CASMO5 are:

- The two-dimensional transport solution is based on the Method of Characteristics (MoC) with a linear source approximation.
- The multigroup energy discretization can be carried out in a number of different energy group structures, with the finest structure using 586 groups and the default for the MoC calculation using 19 groups for UO_2 fuel and 35 groups for MOX.
- Nuclear data for CASMO5 are collected in a library containing microscopic cross sections in 586 energy groups. Neutron energies cover the range from 10^{-5} eV to 20 MeV.
- CASMO5 can accommodate non-symmetric fuel assemblies. It can perform the calculations in half, quadrant, or octant symmetry.
- Absorber rods or water holes covering 1x1, 2x2, 3x3, or 4x4 pin cell positions are allowed within the assembly.
- Thermal expansion of dimensions and densities is performed.
- Effective resonance cross sections are calculated individually for each fuel pin.

- Microscopic depletion is calculated in each fuel and burnable absorber pin.
- The neutron transport and burnup calculations are coupled via a predictor-corrector approach which greatly improves accuracy. This is particularly important when burnable poison rods are involved. A special quadratic depletion model is used for lattices containing gadolinium. The burnup equations are solved with the Chebyshev Rational Approximation Method (CRAM).
- CASMO5 generates output edits of few-group cross sections and reaction rates for any region of the assembly. An ASCII card image file is created for linking to various diffusion theory core analysis programs, e.g., CMSLINK/SIMULATE.
- Reflector calculations are performed and discontinuity factors are calculated at the assembly boundaries and for reflector regions.
- CASMO5 can perform an 18-group gamma transport calculation if required.
- Multi-assembly calculations in CASMO5 are performed using the same transport theory methodology (Method of Characteristics) as the single assembly calculations.

To generate the neutronic data needed for use in SIMULATE5, a series of CASMO5 depletions and branch cases are required. This series of calculations is defined within the CMS5 system as the "SIMULATE5 Case Matrix." This case matrix consists of a series of depletions and instantaneous branch cases versus exposure as a function of varied boron concentrations, moderator temperature, fuel temperature, and shutdown cooling time, as well as cases with control rods and without removable burnable poison in the guide tube locations.

The CASMO5 neutron data library is based on ENDF/B-VII.1 data files (supplemented with TENDL-2012 data) and was processed with NJOY-94.105 [2] and NJOY-2012.8 [3]. In addition, other auxiliary Studsvik Scandpower programs were used to calculate cross sections for complex materials and to extract and handle decay constants, fission yields, fission spectra, and delayed neutron data. A full description of the library is available in the CASMO5 User's Manual [4].

2.2.2 CMSLINK5

CMSLINK5 is a linking code that processes CASMO5 Card Image files into a binary formatted nuclear data library for use by SIMULATE5 or, SIMULATE-3. The code collects the following data from CASMO5 Card Image files:

- Multigroup macroscopic and microscopic nodal cross sections
- Multigroup submesh macroscopic cross sections
- Detector data
- Pin power reconstruction data
- Kinetics data
- Isotopics data
- Spontaneous fission data

CMSLINK5 reads the card image files created by CASMO5 and creates a binary library for SIMULATE5. It is capable of processing data for the following segment types:

- Standard PWR segments with and without burnable poison
- Pulled and reinserted burnable poison for PWR segments
- Standard PWR reflector segments
- Scoping libraries

The data functional dependencies (case matrices) which depend on the reactor type are predefined in the code. Additional detail on the functionalization can be found in the CMSLINK5 User's Manual [5].

The library functionalization used for the macroscopic cross sections is used for the fission product data and discontinuity factors as well. The pin library which includes pin peaking, kinetics, isotopic, and detector data is written for each fuel segment by default. The one-dimensional tables of these parameters are determined by the program.

2.2.3 SIMULATE5

SIMULATE5 [6, 7] is a next generation multi-group analytical nodal code for the steady-state analysis of both PWRs and BWRs. The key features of SIMULATE5 are:

- Pin power reconstruction
- True representation of each fuel assembly in the axial and radial directions
- Explicit representation of the reflector region and PWR baffle
- Expanded cross section modeling capabilities
- Automatic geometry expansion
- Handles fuel with axially dependent thermal hydraulic characteristics

SIMULATE5 solves the multi-group diffusion or, optionally, the simplified P3 transport equations. Cross sections are described by a hybrid microscopic-macroscopic model that includes 50 isotopes (17 actinides and 30+ fission products and burnable absorbers).

SIMULATE5 cross section input is provided from CASMO5 with linkage through CMSLINK5. CMSLINK5 creates a master binary library containing partial cross sections for use by SIMULATE5. The partial cross sections can each be a function of up to three variables (e.g., exposure, fuel temperature, moderator temperature, control rod, enrichment, etc.).

SIMULATE5 creates a runtime library from the master library based on the cross sections being requested by the input. This capability allows the user to maintain one master library that contains all cross section information.

Each assembly in the core is represented in great detail both axially and radially. In the axial direction, SIMULATE5 explicitly treats the heterogeneities due to spacers, control rods, enrichment/burnable absorber zoning and staggered assembly heights. In the radial direction, the fuel assembly is divided into NxN heterogeneous radial submesh regions per node. The pin powers/fluxes and the detector responses are computed based on the fine scale solution obtained by the axial homogenization and radial submesh models.

SIMULATE5's PWR thermal hydraulics model treats the region from lower to upper tie plate. The PWR core portion of the thermal hydraulics model is treated with each assembly having an active channel and a number of parallel bypass channels. For each axial node of a channel, the total mixture mass, steam mass, mixture enthalpy, and momentum balance equations are solved (a four-equation model). The three dimensional fuel temperatures are computed in the thermal hydraulics module by solving the radial Fourier heat conduction equation. Thermodynamic quantities are evaluated using the NIST/ASME steam/water function library.

2.2.4 References

1. B. Haugh, R. M. Ferrer, and J.D. Rhodes, "CASMO5 PWR Methods and Validation Report", SSP-14-P01/012-R Rev 1, Waltham, MA, 2015.
2. R. E. MacFarlane and D. W. Muir, "The NJOY Nuclear Data Processing System, Version 91, LA-12740-M," Los Alamos National Laboratory, Los Alamos, 1994.

3. R. E. MacFarlane, D. W. Muir, R. M. Boicourt and A. C. Kahler, "The NJOY Nuclear Data Processing System, Version 2012, LA-UR-12-27079," Los Alamos National Laboratory, Los Alamos, 2012.
4. J.D. Rhodes, R. M. Ferrer, and J. Hykes, “CASMO5 A Fuel Assembly Burnup Program User’s Manual”, SSP-07/431 Rev 8, Waltham, MA, 2013.
5. T. Bahadir, R. M. Ferrer, and J.D. Rhodes, “CMSLINK5 User’s Manual”, SSP-10/437 Rev 5, Waltham, MA, 2015.
6. S. Vanevenhoven, T. Bahadir, and J.D. Rhodes, “SIMULATE5 User’s Manual”, SSP-10/438 Rev 5, Waltham, MA, 2015.
7. T. Bahadir, G. Grandi, R.M. Ferrer and J.D. Rhodes, “SIMULATE5 Methodology”, SSP-10/465 Rev 3, Waltham, MA, 2014.

2.3 Validation and Benchmarking Overview

The validation and benchmarking process for CMS5 is an important part of the software development process. The process is implemented to ensure that each code accurately performs its intended functions while also ensuring the integral CMS5 system performs in the same manner.

The validation and benchmarking process consists of two primary methods of analysis: the comparison to physical measurements and the comparison to higher order computer codes. While the use of physical measurements for comparison is normally the preferred method, the cost and difficulty in obtaining the measurements limits the range of conditions available. The use of higher order code calculations and computational benchmarks also allows one to study the mechanics of the codes as well as to help ensure proper method implementation over the full range of conditions.

This approach provides the developers and analysts with the data needed to determine if any bias, trends or other anomalies appear in the code results.

This section discusses the process used for validation in support of the Topical Report. The purpose is to convey the range of work, not to present all results exhaustively. Some results are shown as representative or supporting other conclusions or Nuclear Uncertainty Factor's (NUF's) discussed in Section 3.

2.3.1 Measurement Comparisons

Two categories of measurement comparisons are presented in this section. The first category is critical experiments, and second is measured depleted fuel isotopic compositions from post irradiation examinations.

The majority of the measurement comparisons discussed here use CASMO5 results. The CASMO5 code is the data engine for the CMS5 system and it is essential that the reactivity, reaction rate, and isotopic burnup predictions are of sufficient fidelity to allow the code system as a whole to have acceptable accuracy.

Additionally, SIMULATE5 fuel temperature predictions are compared against in-core measurements.

2.3.1.1 Critical Experiments

CASMO5 has been compared against 160 critical configurations in support of this Topical Report. The configurations include small core, fuel storage, and reflector type geometries with a wide range of materials. The results compare both the resulting reactivity / eigenvalue results and fission rate results where available.

The experimental comparisons documented in [1] were chosen as a representative range of high pedigree tests that demonstrate as many types of PWR fuel geometries and materials as possible. The following experiments were analyzed:

- BAW-1810 [2]
- BAW-1484 [3]
- DIMPLE Cores S06A and S06B [4]
- KRITZ3 [5]
- TCA Reflector Critical [6]

The results of the comparisons showed good agreement between eigenvalues calculated in CASMO5 and the critical configurations without significant trends or biases noted.

Fission rate results are available for the BAW-1810, DIMPLE, and KRITZ3 experiments and also show good agreement. These results are used to produce the supporting CASMO5 to measurement pin-to-box uncertainty discussed in Section 3.5.7.

Some limited information on the mean neutron lifetime (l*) and the effective delayed neutron constant (β) are provided from the TCA reflector critical and show very good agreement between CASMO5 and measurement.

2.3.1.2 Isotopic Measurements

CASMO5 has been compared against hundreds of isotopic samples in support of this Topical Report. The data encompasses various regions of operating PWR cores including the presence of burnable absorbers.

The isotopic measurement comparisons documented in [1] were chosen for their direct applicability to PWR predictions since the samples came from operating reactors. The following benchmark data sets were analyzed:

- Yankee Rowe [7, 8]
- JAERI PWR Isotopic Benchmark [9, 10]

2.3.1.2.1 Yankee Rowe Measurements

The Atomic Power Division of Westinghouse destructively analyzed samples from several depleted PWR fuel pins of Yankee Rowe to measure nuclide composition for the purpose of verification of depletion codes.

This data was chosen as it offers a large number of data points within the same reactor core. This is not typical of available isotopic data.

The predictions are based on single assembly calculations depleted unrodded with a power history corresponding to core average conditions over the cycles containing the measured assemblies, including outages at zero power. The power levels for specific sample locations can differ significantly and these early cores of Yankee Rowe were operated at 0 ppm boron using control rods at power.

Isotopic concentrations in pins located far from the effects of the control blades/followers and corresponding variation in pin pitch are referred to as 'asymptotic'. Concentrations for pins adjacent to such components are referred to as 'perturbed', and pins located in regions in between are 'intermediate'.

In general the results [1] show that CASMO5 can reasonably predict the isotopic burnup trends of PWR fuel. A sample of the results are shown in Figure 2-1 and Figure 2-2 for U235 and Pu239 respectively. These are important isotopes and show the large number of samples compared.

Figure 2-1: Yankee Rowe U235 CASMO5 Comparison to Measurement

Figure 2-2: Yankee Rowe Pu239 CASMO5 Comparison to Measurement

The Japan Atomic Energy Research Institute destructively analyzed samples from several depleted PWR and BWR fuel pins to measure nuclide composition for the purpose of verification of depletion codes.

An analysis was performed in CASMO5 [1] to generate isotopic data for comparison to the measurements. These predictions are based on single assembly calculations depleted with power histories that correspond to the sample histories. Control rod history effects are not important for these cores.

In general the results demonstrate that CASMO5 can reasonably predict the isotopic burnup of PWR fuel including fuel containing gadolinia.

2.3.1.3 HALDEN Fuel Temperature Measurements.

The fuel temperature model present in SIMULATE5 performs on the fly calculations during the execution of the code. The code uses the predicted nodal-average fuel temperatures to look up the appropriate cross-sections as well as to provide data for the thermal hydraulic model. Thus it was important to benchmark these predictions against experimental measurements.

The validation documented in [11] compares SIMULATE5 fuel temperature predictions against measurements from the Halden boiling water reactor for many fuel rods during the operation and depletion of the core. A wide variety of pin types were included in the Halden measurements; eight of those rods are analyzed for the validation. The final burnup of the rods analyzed range from 12 to 60 MWd/kgU. Because of differences in linear heat generation, the center-line temperatures of these rods range from 800 to 1550 K.

SIMULATE5 fuel temperature predictions are within { } for most of the rods. For two of the rods SIMULATE5 has larger differences, up to about { }. Given the modeling approximations and adjustments in the measured data, the comparisons show good agreement at zero exposure as well as for the increasing trend in the center-line fuel temperature with burnup. This demonstrates the adequacy of the model in SIMULATE5.

2.3.2 Higher-Order Code Comparisons

Higher-order code comparisons are used to identify code-to-code trends and biases that may signal deficiencies in the code system. Additionally these comparisons extend the range of benchmarking to materials and configurations that are not available in the experimental data.

This method has been applied across the CMS5 system to ensure consistency of the results and to ensure that each component of the computational uncertainty is examined.

2.3.2.1 CASMO5 to MCNP

For the CASMO5 validation and benchmarking [1] MCNP6 [12] is the higher-order code used for comparisons. It is used to examine any code to code trend using the same nuclear data to ensure robust computational methods. It is also used to produce additional pin-by-pin power data to support the use of Integral Fuel Burnable Absorber (IFBA) fission rates in the NUF generation as discussed in Section 3.5.7.

2.3.2.1.1 CASMO5 to MCNP6 Lattice Reactivity Comparisons

Comparison calculations have been made in [1], between CASMO5 and MCNP6 to examine the reactivity effects of different operating conditions. These include Doppler temperature defects, moderator temperature defects, soluble boron worth, and control rod worth.

The analysis also supplements the measured data compared earlier. Given that experimental data is not available over the full range of PWR operation, the use of continuous-energy Monte Carlo is the next best reference.

The two codes are compared with consistent nuclear data (i.e. ENDF/B-VII.1) to provide insight into any significant modeling differences. The results show reasonable agreement between CASMO5 and MCNP6.

The Moderator Temperature and Doppler defects are compared in Figure 2-3 and Figure 2-4 respectively and show little trend. No other trends were noted with: ITC, rod worth, or boron worth.

The lattice reactivity comparisons with MCNP6 show there are no large systematic biases that need to be addressed before providing the CASMO5 data to SIMULATE5.

Additional comparisons for IFBA are created as there is an absence of available critical experiment data. The comparisons between CASMO5 to MCNP6 are used to show that CASMO5 calculations with IFBA perform as well as other materials and support the generation of the CASMO5-to-measurement component used as part of the NUF generation process.

Figure 2-3: CASMO5 vs. MCNP6 Moderator Temperature Defect

Figure 2-4: CASMO5 vs. MCNP6 Doppler Defect

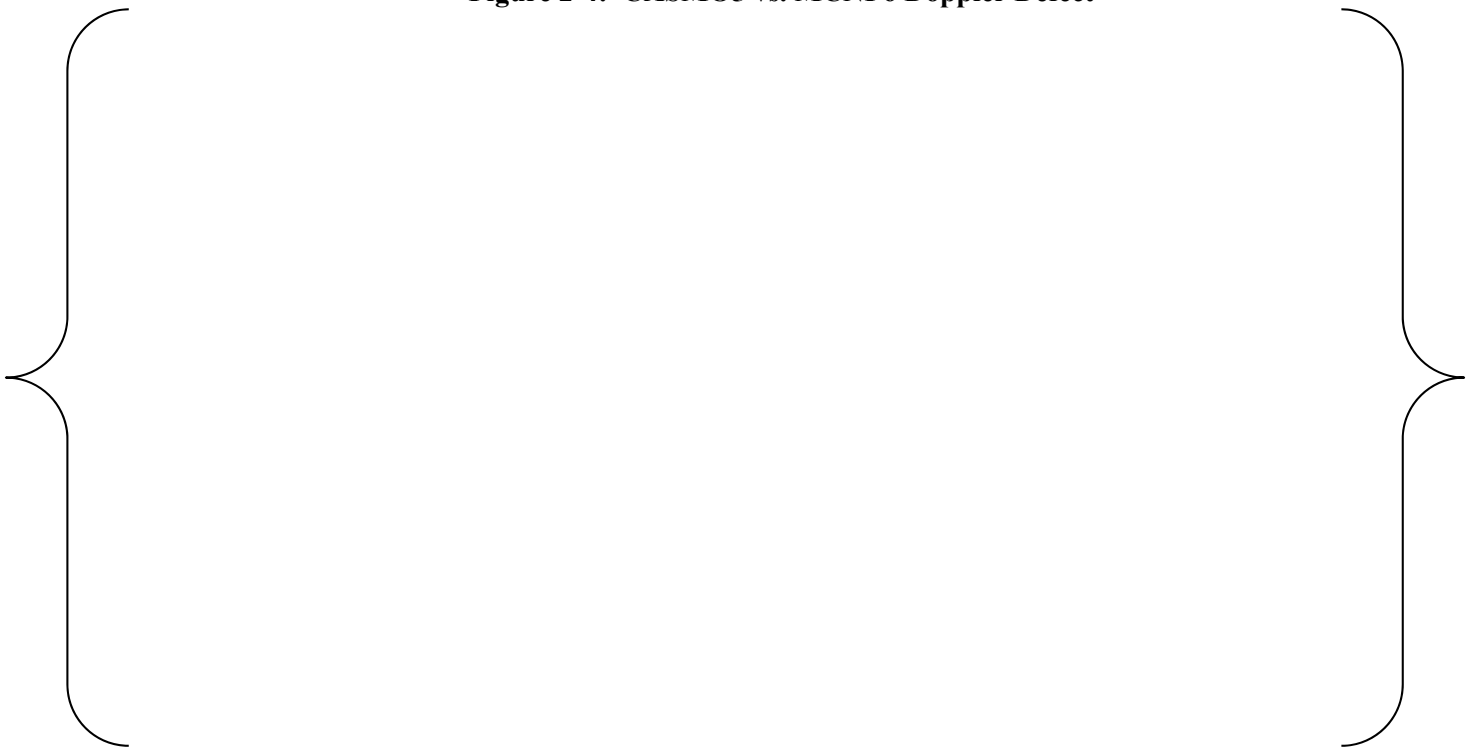

2.3.2.1.2 CASMO5 C5G7 Benchmark

The OECD C5G7 benchmark [13] was performed to verify the adequacy of the transport solution within CASMO5. This benchmark is independent of the ENDF/B-VII.1 library as this benchmark supplied the associated cross-section data used in the calculation. The results reported in [1] show good agreement between CASMO5 and the reference for both eigenvalue and pin powers.

2.3.2.2 CASMO5 to SIMULATE5

After establishing the accuracy of CASMO5 using the above-mentioned tests, CASMO5 is used as the higher-order code to generate reference solutions to compare against the nodal code SIMULATE5. This strategy is used for examining the last three components of the code system: the standard case matrix, the SIMULATE5 nodal code, and pin-to-box uncertainties needed to support the NUF development.

2.3.2.2.1 Standard Case Matrix Assessment

The adequacy of the case matrix is assessed [14] using a technique where exact statepoint calculations from CASMO5 are performed over the PWR operating regime including conditions representative of inputs to the safety analysis. These are then compared to SIMULATE5 results where the standard case matrix was run and cross-sections are interpolated from the library generated in CMSLINK5. The resulting differences are examined to ensure the expected performance and adequacy of the case matrix and library. The results of the analysis show that the case matrix is robust and sufficient for a PWR core.

2.3.2.2.2 SIMULATE5 Pin-to-Box Uncertainty

The purpose of this analysis [15] was to establish the uncertainty in the pin-to-box ratios computed by SIMULATE5. A fuel pin's pin-to-box ratio is defined as the ratio of the pin power to the assembly average power.

Because the pin powers in a PWR fuel assembly cannot be measured directly, a high fidelity calculation is used in place of measurements. In this case, multi-assembly CASMO5 calculations serve as the high fidelity references. The accuracy of CASMO5's pin by pin fission rate distributions has been validated against MCNP6 and critical measurements [1].

The uncertainty on the SIMULATE5 pin-to-box ratios is established by examining a broad range of potential configurations for a 2 by 2 lattice colorset, considering combinations of lattice types, enrichments, boron concentrations, and integral and removable features. Each 2x2 colorset has two fresh and two once burnt assemblies. The once burnt assemblies are taken from single assembly lattices depleted to 20 MWd/kgU. The depleted assemblies did not have removable burnable poisons (BPs) or control rods (CRs). The fresh fuel optionally includes BPs or CRs.

The resulting differences are used in support of the NUFs in Section 3.5.7.

2.3.2.2.3 BEAVRS Benchmark

Further benchmarking of SIMULATE5 is done by using the BEAVRS [16] model. This was done by performing 2D CASMO5 MxN calculations and consistent 2D SIMULATE5 calculations with depletion. The higher order transport methods of CASMO5 are used to assess the accuracy of SIMULATE5 for reactivity, power distributions, rod worth and isothermal temperature coefficient (ITC). These results were consistent with expectations and show no biases or deviations that needed to be addressed.

2.3.3 References

1. B. Haugh, R. M. Ferrer, and J.D. Rhodes, “CASMO5 PWR Methods and Validation Report”, SSP-14-P01/012-R Rev 1, Waltham, MA, 2015.

2. L.W. Lewman, “Urania-Gadolinia: Nuclear Model Development and Critical Experiment Benchmark,” B&W 1810, DOE/ET/34212-41, Babcock & Wilcox, 1984.
3. M.N. Baldwin et. al., “Critical Experiments Supporting Close Proximity Water Storage of Power Reactor Fuel,” BAW-1484-7, Babcock & Wilcox, 1979.
4. NEA/NSC/DOC(95)03/IV, LEU-COMP-THERM-055, “Light-Water Moderated and Reflected Low-Enriched Uranium (3 wt.% U235) Dioxide Rod Lattices”.
5. E. Johansson *et al.*, “KRITZ-3 Experiments”, Internal Report, AB Atomenergi, Studsvik, Sweden, 1973.
6. Y Tahara *et al.*, “Reactivity Effect of Iron Reflector in LWR Cores”, *Nuclear Science and Technology*, Vol. 28, No.2, p. 102-111.
7. R. J. Nodvik *et al.*, “Evaluation of Mass Spectrometric and Radiochemical Analyses of Yankee Core 1 Spent Fuel”, WCAP-6068, 1966.
8. R. J. Nodvik *et al.* , “Supplementary Report on Evaluation of Mass Spectrometric and Radiochemical Analyses of Yankee Core I Spent Fuel, including Isotopes of Elements Thorium through Curium”, TID 4500, WCAP-6086, 1969.
9. K. Suyama *et al.* , “Re-evaluation of Assay Data of Spent Nuclear Fuel Obtained at Japan Atomic Energy Research Institute for Validation of Burnup Calculation Code Systems,” *Annals of Nuclear Energy*, Vol. 38, p. 930 941, 2011.
10. K. Suyama *et al.* , “Nuclide Composition Benchmark Data Set for Verifying Burnup Codes on Spent Light Water Reactor Fuels,” Nuclear Technology, Vol 137, p 111-126, 2002
11. J. Hykes, R.M. Ferrer, “Benchmarking SIMULATE5 with Halden Fuel Temperature Measurements”, SSP-14-P01/022-C, Waltham, MA, 2015.
12. T. Goorley*, et al*., “Initial MCNP6 Release Overview”, *Nuclear Technology*, **180**, pp 298-315 (Dec 2012).
13. NEA/NSC/DOC(2003)16, "Benchmark on Deterministic Transport Calculations Without Spatial Homogenisation, A 2-D/3-D MOX Fuel Assembly Benchmark”, 2003.
14. B. Haugh, D. Dean, “S5C Case Matrix Assessment”, SSP-14-P01/020-C, Waltham, MA, 2015.
15. J. Hykes, B. Haugh, “SIMULATE5 Pin-To-Box Uncertainties”, SSP-14-P01/016-C Rev. 1, Waltham, MA, 2015.
16. E. Wehlage, M. Kruners, “Benchmarking the SIMULATE5 BEAVRS Model with CASMO5 MxN”, SSP-14-P01/023-C, Waltham MA, 2015.

2.4 Conclusion

The CMS5 code system has been described in Section 2.2 allowing the reader to understand the basic functions and interactions of the code system.

An overview of the validation and benchmarking process used to demonstrate the CMS5 code system is sufficient for application to PWR core analysis has been presented in Section 2.3. It demonstrates the robust software development process used at Studsvik Scandpower to ensure proper code function from CASMO5 through SIMULATE5.

The validation and benchmarking process has been accomplished by comparing against 160 critical configurations that span the range of PWR lattice geometries, materials, and conditions. The inclusion of isotopics measurements shows CMS5 has an appropriate depletion scheme and data to handle the burnup predictions of PWR cores. The use of higher-order code comparisons and computational benchmarks ensure the entire range of conditions are examined even when measurements are not available. No fundamental trends or biases were observed that required any changes ahead of the code system application in analyzing operating PWRs.

3. CMS Nuclear Uncertainty Factor Methodology

3.1 Introduction

3.1.1 Purpose

The purpose of this section is to present a methodology by which appropriate Nuclear Uncertainty Factors (NUFs) (also called "uncertainty factors") can be developed to use in conjunction with the CMS5 software system. These factors are the basis of Nuclear Reliability Factors (NRFs), which are applied to predicted CMS values to conservatively estimate a particular core condition.

3.1.2 Background

There are several instances in which it is either desirable or necessary to quantify the uncertainty of a particular prediction from a nuclear physics design tool such as CMS5. In many cases these predictions are used as part of a safety analysis / core reload methodology, startup physics / initial testing program, or generation of inputs to processes that satisfy plant licensing or design bases, such as shutdown margin calculations.

For previous versions of the CMS system, individual licensees have submitted their own reports for NRC review and approval for the method of determining these CMS Nuclear Uncertainty Factors (these uncertainty factors are known by many names, but in this report they will henceforth be known as NUFs).

The following is a partial list of NRC reviewed and approved reports for previous main versions of the CMS software system:

1. "Qualification of the Studsvik Core Management System Reactor Physics Methods for Application to North Anna and Surry Power stations" [1]
2. "Oconee Nuclear Design Methodology Using CASMO-4 / SIMULATE-3" [2]
3. "PWR Reactor Physics Methodology Using CASMO-4/SIMULATE-3" [3]

The submittals listed above have common methodological elements:

1. a method to compare predictions to measurements
2. a method to qualify the distribution of the differences
3. a statistical method to develop the NUFs from the observed differences between measured and predicted values

Another common element of the above reports is that they are tied to particular plants/units that are operated by their respective licensees. This report reintroduces many concepts and methods that have already been reviewed and approved by the NRC and presents them as a generic methodology appropriate for the class of plants and applications specified in the Scope section. While much of the methodologies of Reference [1] have been included (with permission from the licensee) to form the core of this methodology, an effort has been made to adopt best practices from all available resources.

3.1.3 Scope

- This NUF methodology is applicable for pressurized water reactor (PWR) plant designs.
- This NUF methodology is applicable to square fuel lattice designs with regularly spaced arrays of fuel pins.
- This NUF methodology is applicable to only low enriched uranium (LEU) fuel assemblies / cores, **NOT** to Mixed Oxide (MOX) fuel assemblies / cores.
- This NUF methodology is independent of any particular CASMO5, CMSLINK5, SIMULATE5, or base cross section (ENDF, JEFF) version, sub-version, or modification. See Section 3.7 for description of the change methodology that governs this software and uncertainty factor methodology.

3.1.4 References

1. R. A. Hall et al., Dominion, "Qualification of the Studsvik Core Management System Reactor Physics Methods for Application to North Anna and Surry Power Stations", DOM-NAF-1-Rev 0.0-P-A, NRC Safety Evaluation Date: March 2003, **NRC Accession Number: ML031690108.**
2. Duke Energy Carolinas, "Oconee Nuclear Design Methodology Using CASMO-4 / SIMULATE-3", DPC-NE-1006-A, Revision 0a, NRC Safety Evaluation Date: August 2011, **NRC Accession Number: ML101580106.**
3. S.G. Zimmerman et al., Arizona Public Service Company, "PWR Reactor Physics Methodology Using CASMO-4/SIMULATE-3", Enclosure 3 to Reference [4], **NRC Accession Number: ML010440094.**
4. Arizona Public Service Company, "Palo Verde Nuclear Generating Station (PVNGS) Units 1,2 and 3 – Request for Amendment to Technical Specification 5.6.5, Core Operating Limits Report (COLR) (CASMO-4/SIMULATE-3)", Letter dated June, 2000, **NRC Accession Number: ML003723799.**

3.2 Methodology Overview

3.2.1 Nuclear Uncertainty Factor Definition

The Nuclear Uncertainty Factor (NUF) is defined as the calculational uncertainty for a core physics model parameter derived from a statistical analysis (where practical) of measurements and predictions of the parameter. If measurements are not available in sufficient quality or quantity to determine the NUF directly, comparisons can be made to higher order calculations, or the uncertainty can be inferred indirectly using observations of dependent quantities.

The core physics parameters discussed in this methodology section are grouped into two categories.

3.2.2 Nuclear Reliability Factor Definition

The Nuclear Reliability Factor (NRF) is defined as the allowance to be applied to a safety related core physics model design calculation and is chosen to be equally conservative or more conservative than the corresponding NUF. This quantity is typically a convenient number that bounds the NUF. For example if the integral control rod worth NUF Upper and Lower values are 1.074 and 0.938 respectively, the corresponding upper and lower NRF could be set to 1.10, 0.90.

3.2.3 One-Sided Tolerance Limit Statistical Analysis

The first category is a set of physics parameters for which it is possible to use a rigorous and well defined statistical method involving historical plant measurements (and in some cases higher-order codes or critical experiments) and CMS5 predictions to determine appropriate NUFs. The physics parameters in this category are some of the most important and widely used parameters in PWR core design / safety analysis:

- Overall core reactivity
- Integral control rod worth
- Peak differential control rod worth
- Isothermal temperature coefficient
- 2D peak pin factor, i.e. “enthalpy rise hot channel factor” ($F\Delta H$ / Fr)
- 3D peak pin factor, i.e. “heat flux hot channel factor” (FQ)

For this category of physics parameter, no specific value is presented for review and approval. Licensees are allowed to exercise this methodology to generate unit / plant specific NUFs assuming their particular application falls within the Scope of this document and assuming they have access to a sufficient amount of benchmark quality measured data.

Since not all licensees can (or will want to) exercise this methodology, Section 4.0 of this report includes a demonstration involving over 60 cycles of measured data from seven PWR nuclear units. This demonstration fulfils the following purposes:

1. Section 4 presents a traditional benchmark of how well the CMS5 system predicts core characteristics.
2. Section 4 also provides a demonstration of the One-Sided Tolerance Limit Statistical Analysis methodology described in Section 3.
3. Finally Section 4 generates generic PWR NUFs that licensees ***may*** use without deriving their own NUFs **if** their nuclear units and particular application are within the bounds described in Section 3.1.3.

3.2.4 Engineering / Physical Arguments

For those physics parameters for which it is difficult or impossible to generate difference data, or for which the measurement uncertainty component of the difference data dominates, appropriate NUFs are presented

based upon engineering arguments. For these physics parameters a specific value for the NUF/NRF is presented for review and approval. This category includes physics parameters that are used less often in typical reload/startup testing/safety analysis applications:

- Differential Boron Worth
- Doppler Temperature / Power Coefficient
- Kinetics Parameters (Delayed Neutron and Prompt Neutron Lifetime)

Appropriately conservative NRFs for these physics parameters are determined by examining other closely related parameters (e.g. critical boron for boron worth), by modeling plant operational transients, or by relying on NRF values that have been previously reviewed and approved. For some of these parameters, supporting data from Section 4.0 is cited. No mechanism is presented to allow licensees to change these NRFs within the context of this topical report methodology.

3.3 One-Sided Tolerance Limit Statistical Analysis

3.3.1 Introduction

The one-sided tolerance limit statistical analysis method is a rigorous method of determining conservative Nuclear Uncertainty Factors for those physics parameters for which it is possible to compare CMS5 predictions with measurements and/or higher order codes.

The basic methodology steps are:

1. For a given physics parameter, compute a set of differences between prediction and measurement.
2. Characterize the set of differences as being either :
    a. Normally distributed.
    b. Non-normally (non-parametric) distributed.
3. Construct one-sided statistical tolerance limits using:
    a. Standard deviation multipliers if the difference data is normally distributed.
    b. Sorted data non-parametric method if the difference data is not normally distributed.
4. Convert the one-sided statistical tolerance limits into Nuclear Uncertainty Factors.

Each of these steps is described in greater detail in the following sections.

It is important to note that when determining a NUF using statistical analysis involving the comparisons of predictions and measurements, measurement uncertainty is inherently included in the statistically determined NUF. The inclusion of modest amounts of measurement uncertainty in the difference data is tolerable as it helps assure the predicted uncertainty factors are conservative. However if the measurement uncertainty is too large it can lead to unreasonably large estimates of model predictive uncertainty, for example the case of differential boron worth as described in Section 3.6.1.

3.3.2 Statistical Tolerance Limits

To determine a conservative NUF to apply to a particular uncertainty factor, *statistical tolerance limits* are developed for those physics parameters for which it is possible to determine a difference between prediction and measurement (or between a prediction and higher-order codes in some cases).

As defined in Reference [1]:

"S*tatistical tolerance limits* for a given population are limits within which we expect a stated proportion of the population to lie with respect to some measurable characteristic."

In this case the population of interest is the set of computed differences between CMS5 predictions and plant measurements. Of course the only samples available to us are the historical measurements already taken; it is from this historical database that tolerance limits (and then uncertainty factors) are constructed to use for future predictions.

A note of caution, *statistical tolerance limits* are distinct from *engineering tolerance limits*, defined thus (from Reference [1]):

"*Engineering tolerance limits* are specified outer limits of acceptability with respect to some characteristic usually prescribed by a design engineer."

3.3.3 95/95 One-Sided Tolerance Limits

Several decisions must be made when using statistical tolerance limits, including:

- Should the test be one-sided or two-sided?
- What percentage of the population is intended to be bounded?
- Since a sample is taken from the population, what level of confidence should be selected?

A 95/95 one-sided tolerance limit is chosen for this application. A one-sided tolerance is acceptable for the physics parameters of interest (such as control rod worth) because the NUF is applied in the conservative direction for each analysis scenario. A concern of simultaneous over-prediction and under-prediction does not apply to a parameter for a given event; that is, a key parameter used in a particular safety event will either be conservative in the high direction or low direction, but never both at the same time. The NUF that is derived from the tolerance limit is applied to a model prediction such that the result will be conservative compared to the corresponding measurement for 95% of the population with a 95% confidence level.

The one-sided tolerance limit is determined using different methods depending on whether or not the data set is normally distributed. To test for normality the difference data must first be obtained and the summary statistics (mean, sample standard deviation) of the data set must be computed.

3.3.4 Difference Data

The difference between a predicted value and corresponding reference value (measurement or higher-order code) is calculated as either:

$$Absolute\ Difference = (Prediction - Reference) \tag{3.1}$$

or

$$Percent\ Difference = \frac{(Prediction - Reference)}{Prediction} \times 100\% \tag{3.2}$$

In the case of percent relative differences, the difference is divided by the prediction because ultimately the NUF that is derived from the difference data will be multiplied by a predicted value.

3.3.5 Summary Statistics

The average as discussed in this report is the arithmetic mean shown in equation (3.3).

$$Average = \overline{X} = \frac{1}{N}\sum_{i=1}^{N} a_i \tag{3.3}$$

Where a_i is a calculated difference for data point i.

The standard deviation is used to measure the spread of the data from the mean. The sample standard deviation is used in this report, often called the ‘n-1’ method.

$$Sample\ Standard\ Deviation = s = \sqrt{\frac{1}{N-1}\sum_{i=1}^{N}(X_i - \overline{X})^2} \tag{3.4}$$

Where $\overline{X}$ is the average of the quantity in the set as described by equation (3.3).

3.3.6 Test for Normality

The Shapiro-Wilk *W* [2] test is used to determine whether or not the difference data can be considered to come from a normal distribution. The particular implementation of the Shapiro-Wilk test used in this methodology is the AS R94 (Royston, 1995) implementation that allows the test to be used for any sample size *n* in the range $3 \leq n \leq 5000$. Reference [3] provides a description of the historical evolution of the Shapiro-Wilk test from the original ANSI implementation to the AS R94 implementation and also concludes that the Shapiro-Wilk test is the most powerful test for all types of distribution and sample sizes versus other popular tests such as Kolmogorov-Smirnov, Lilliefors, and Anderson-Darling. The AS R94 implementation of Shapiro-Wilk is included in statistics software packages such as R and Dataplot.

The significance level chosen for this normality test is $\alpha = 0.01$. This significance level is consistent with the assumption that the physics parameter differences should typically follow a normal distribution and that we are unwilling to reject the null hypothesis of normality unjustly. This significance level is the same as used in Regulatory Guide 1.126 [4]. Although Regulatory Guide 1.126 is concerned with an entirely different topic (fuel densification), the statistical methods described in it have been employed in previously reviewed and approved physics methods applications [5][6].

3.3.7 Determining Tolerance Limits Assuming Normality

If the difference data set is determined to be normal, then the lower and upper tolerance limits can be computed from the following formulas which are described in References [4] and [7].

$$Lower\ Tolerance\ Limit = TL_L = \overline{X} - (K \times s) \tag{3.5}$$

$$Upper\ Tolerance\ Limit = TL_U = \overline{X} + (K \times s) \tag{3.6}$$

where:

$\overline{X}$ = the average of the difference data

s = the sample standard deviation of the difference data

K = one-sided tolerance multiplier.

From Reference [7], *K* is most accurately determined for all sample sizes from the following equation:

$$K = \frac{t(\gamma, N-1, \delta)}{\sqrt{N}} \tag{3.7}$$

where:

$t(\gamma, N-1, \delta)$ = inverse cumulative distribution function for the non-central *t* distribution

γ = confidence level (0.95)

N = number of observations

δ = non-centrality parameter calculated as:

$$\delta = z(p)\sqrt{N} \tag{3.8}$$

where:

p = proportion of the population to be bounded (0.95)

z(p) = cumulative normal distribution function for example $z(p = 0.95) \approx 1.645$

N = number of observations

Table 3-1 presents calculated *K* values using equation (3.7) for the same number of observation (N) values listed in Regulatory Guide 1.126 [4]. The calculated values agree very closely with those listed in the Regulatory Guide (Table 1 of Reference [4]).

Table 3-1: Examples of Multiplier (*K*) Used To Determine Tolerance Limits for Normally Distributed Data

Number of Observations (N)	Tolerance Multiplier (*K*)
4	5.14
5	4.20
6	3.71
7	3.40
8	3.19
9	3.03
10	2.91
11	2.81
12	2.74
15	2.57
20	2.40
25	2.29
30	2.22
40	2.13
60	2.02
100	1.93
200	1.84
500	1.76
1000000	1.65

3.3.8 Determining Non-Parametric Tolerance Limits

If the difference data set is determined to be non-normal, then the lower and upper tolerance limits are determined from the non-parametric ranking of Somerville [8] referenced in Regulatory Guide 1.126 [4]. The Somerville equation of interest is:

$$\gamma \leq I_{1-P}(m, N-m+1) \tag{3.9}$$

where:

γ = the one-sided confidence level (0.95)

I = regularized version of the incomplete Beta function (also known as the cumulative distribution function of the beta distribution)

P = proportion of the population bounded by the m^{th} value

N = number of observations

m = m^{th} largest rank in the sorted sample

Bounding 95% of the population with a 95% confidence level, the equation becomes:

$$0.95 \leq I_{0.05}(m, N-m+1) \tag{3.10}$$

This equation is typically solved by iterating on m for a given number of observations N. The largest integer value of m that satisfies the above relationship is the value of interest.

Note that in the original Somerville reference [8] that the function I_{1-P} is described as the "incomplete Beta function"; however based on the notation and usage this function is (in current terminology) referred to as the "regularized incomplete Beta function" (sometimes shortened to "regularized Beta function", or the "BETADIST" function in Excel).

Table 3-2 provides an example of m values for a set of N observations.

The difference data must be sorted (i.e. most negative difference to most positive difference). If a negative tolerance limit is desired, the m^{th} value counted from the most negative side of the list is selected and becomes the lower tolerance limit. The positive tolerance limit would be selected in the same way, counting m values from the most positive value of the sorted list.

Table 3-2: Examples of sorted list m values to determine Tolerance Limits for Non-normally Distributed Data

Number of Observations (N)	m^{th} value
60	1
80	1
90	1
95	2
100	2
120	2
130	3
140	3
150	3
170	4
200	5
300	9
400	13
500	17
600	21
700	26
800	30
900	35
1000	39
2000	84
5000	225
10000	464
100000	4887
200000	9840

3.3.9 Determination of Nuclear Uncertainty Factors from Tolerance Limits

Under the definitions presented in Section 3.3.4, the sign convention is such that a positive value indicates over-prediction of the magnitude of a parameter by CMS5, and a negative value indicates under-prediction by CMS5. The appropriate interpretation of statistical data is therefore to determine an uncertainty factor in the opposite direction to be applied to CMS5 predictions.

For absolute difference data, the signs of the tolerance limits are simply switched to form the NUFs. For example, if statistically determined tolerance limits for overall core reactivity are -315 pcm to + 345 pcm, then the uncertainty factor to apply to a predicted reactivity value is at least +315 pcm when maximum reactivity is conservative and -345 pcm when minimum reactivity is conservative.

Similarly, statistics given in percent difference are defined as (CMS5 – Reference) / CMS5 in units of percent. The uncertainty factor in this case should be a multiplier on the CMS5 value consistent with this definition. If a tolerance interval for a parameter is indicated to be -5% to +8%, the appropriate multiplier range for CMS5 predictions is 1.05 (when the maximum parameter estimate is desired) and 0.92 (when the minimum parameter estimate is desired).

3.3.10 References

1. M. G. Natrella, “Experimental Statistics”, National Bureau of Standards Handbook 91, p. 1-15, August 1963.
2. “American National Standard Assessment of the Assumption of Normality (Employing Individual Observed Values)”, ANSI N15.15-1974, Approved October 3, 1973, American National Standards Institute.
3. N. M. Razali, Y. B. Wah, “Power comparisons of Shapiro-Wilk, Kolmogorov-Smirnov, Lilliefors and Anderson-Darling tests”, Journal of Statistical Modeling and Analytics, Vol.2 No.1, 21-33, 2011.
4. “An Acceptable Model And Related Statistical Methods for the Analysis of Fuel Densification”, U.S.N.R.C. Regulatory Guide 1.126, Rev. 2, March 2010.
5. R. A. Hall et al., Dominion, “Qualification of the Studsvik Core Management System Reactor Physics Methods for Application to North Anna and Surry Power Stations”, DOM-NAF-1-Rev 0.0-P-A, NRC Safety Evaluation Date: March 2003, **NRC Accession Number: ML031690108.**
6. Duke Energy Carolinas, “Oconee Nuclear Design Methodology Using CASMO-4 / SIMULATE-3”, DPC-NE-1006-A, Revision 0a, NRC Safety Evaluation Date: August 2011, **NRC Accession Number: ML101580106.**
7. NIST/SEMATECH e-Handbook of Statistical Methods, http://www.itl.nist.gov/div898/handbook/, 11/20/2015, Section 7.2.6.3, “Tolerance intervals for a normal distribution”.
8. P.N. Somerville, “Tables for Obtaining Non-Parametric Tolerance Limits”, Ann. Math. Stat. Vol. 29, pp. 599-601 (1958).

3.4 NUFs derived from One-Sided Tolerance Limit Statistical Analysis (non Pin Power)

3.4.1 Introduction

The following sections will detail the derivation of NUFs for the core physics design parameters that lend themselves to the statistical methods described above, excluding the pin power uncertainties. The pin power uncertainties are discussed in their own Section (3.5) due to the additional complexity in determining them.

For each physics parameter typical sources of obtaining the measurements are discussed and any special considerations comparing the measurements to predictions are listed.

3.4.2 Core Reactivity (critical boron concentration)

For PWRs, core wide reactivity agreement between predictions and measurements is often characterized in terms of differences in critical boron concentration (ppm). A potential issue with this approach is that the reactivity worth of a ppm of soluble boron is dependent on fuel enrichment, fuel exposure, presence of competing absorbers, etc. For this methodology, differences in reactivity are expressed in reactivity worth (pcm) using predicted boron worth values to convert from ppm to pcm.

Items for Consideration:

1. Measured boron concentrations from almost any core condition can be used including HZP startup testing through HFP operation, estimated critical conditions, and operational transients.
2. The B^{10} / B atom ratio of any particular boron sample can introduce uncertainty to the comparison if it is not accounted for. CMS5 assumes a default B^{10} / B atom ratio of { } atom percent. Strategies to reduce this uncertainty include:
   2.1. Use boron samples from times where the B^{10} / B atom ratio is known through measurement (mass spectroscopy), and adjust the measurement or prediction to ensure they are on the same B^{10} / B basis.
   2.2. Use boron samples from the end of cycle ($\approx <$ 50 ppm) where any boron worth error due to the B^{10} / B atom ratio being different from that assumed in the prediction is minimized.
   2.3. Correct for B^{10} depletion effects using a depletion model. The most accurate models assume some knowledge of actual leak rates, RCS inventory changes, and the B^{10} / B atom ratio of the various storage tanks (BAST, RWST, etc).
3. Soluble boron measurement uncertainty is introduced by the titration techniques used to analyze the sample. An inferred estimate of this uncertainty is { } from Reference [1].

3.4.3 Integral Control Rod Worth (Individual Banks and Total of All Banks)

Integral rod worth measurements are typically taken during HZP startup physics testing. There are several methods used to measure the bank worths including the boron dilution, rod swap, and dynamic rod worth methods. Integral control rod worth differences are calculated as percent differences.

Items for Consideration:

1. Rod worth measurements depend on a “reactivity computer” or “reactimeter” that uses point kinetics values from a physics code. A correction for kinetics may be needed when comparing measured-to-predicted values when the measurements were made using kinetic parameters from a different physics code.
2. Including percent differences of low worth banks will tend to overestimate the size of the tolerance limit. Bank worth percent differences for measured control rod worths of 300 pcm or less should be excluded from the data set. This cutoff is acceptable because it retains all but the smallest control rod worths in the difference data set and is less than half the rod worth at which the ANSI [1] test criteria switches from a

percentage basis to a reactivity basis (the ANSI standard recommends reporting the larger of 15 % or 100 pcm, so the breakpoint is about 670 pcm).

3.4.4 Peak Differential Control Rod Worth

For control rod banks measured using the boron dilution or the dynamic rod worth method, the differential rod worth (DRW) can be measured. Peak differential control rod worth differences are calculated as percent differences.

Items for Consideration:

1. Rod worth measurements depend on a "reactivity computer" or "reactimeter" that uses point kinetics values from a physics code. A correction for kinetics may be needed when comparing measured-to-predicted values when the measurements were made using kinetic parameters from a different physics code.
2. No distinction is made concerning the rod position at which the peak DRW occurs because the most important use of the DRW is typically for the rod withdrawal from subcritical accident. That accident is terminated after a few seconds and the maximum DRW is usually conservatively assumed to occur for the entire withdrawal sequence. Therefore the peak predicted DRW is compared against the peak measured DRW to generate a single percent difference value per measured control rod.

3.4.5 Isothermal / Moderator Temperature Coefficient

The isothermal temperature coefficient is measured at BOC, HZP as part of startup physics testing. ITC differences are expressed in terms of absolute difference, typically in units of pcm/°F.

Items for Consideration:

1. ITC measurements depend on a "reactivity computer" or "reactimeter" that uses point kinetics values from a physics code. A correction for kinetics may be needed when comparing measured-to-predicted values when the measurements were made using kinetic parameters from a different physics code.
2. Although only the ITC is measured, the same comparison statistics are used for the MTC since the MTC is the main component of the ITC measurements. The Doppler coefficient portion of the ITC is small (between 1 and 2 pcm/°F) and nearly constant at all reactor operating conditions, whereas the MTC component is highly dependent on fuel enrichment, soluble boron concentration, and moderator density.

3.4.6 References

1. "American National Standard Reload Startup Physics Tests for Pressurized Water Reactors", ANSI/ANS-19.6.1-2011, Approved January 2011.

3.5 Peaking Factor NUFs derived from One-Sided Tolerance Limit Statistical Analysis

3.5.1 Introduction

To construct conservative uncertainty factors to apply to pin power predictions, predicted pin powers would ideally be compared directly to measured values. Unfortunately, in most power reactors there is no method available to directly measure individual pin powers. The following sections detail how peaking uncertainty factors can be obtained from the combination of several physical properties.

3.5.2 Predicted Peak Pin Power

SIMULATE5 can compute pin power by two methods:

1. Via the SMX-method where the assembly is divided into NxN submeshes. For each submesh the flux distribution is determined. By superimposing pin power form functions (computed by CASMO5) on the flux, the power of each pin is found.
2. Via the Fourier Flux Expansion method, where the basic geometry unit is not a submesh but an assembly wide node (or, possibly, a quarter-assembly node).

In both cases the Nuclear Uncertainty Factor for peak pin power is determined by combining the uncertainty from two independent components: a “global” power distribution estimator (normalized thimble reaction rate differences) and a “local” heterogeneity estimator (pin-to-box ratio).

The task then is to determine an uncertainty for the predicted assembly power and an uncertainty for the pin-to-box ratio and to combine them together to determine an overall uncertainty for 2D / 3D peaking factor quantities such as FΔH/Fr and FQ.

3.5.3 Thimble Reaction Rates

Thimble reaction rates comparisons are used to determine a conservative approximation of the predicted assembly power uncertainty. It is conservative because it inherently includes not only predicted power uncertainty, but measurement uncertainty and uncertainty associated with reconstructing the predicted thimble reaction rates.

Station flux map data is used for the comparison. For each flux map used in the analysis, measured reaction rates are normalized to the average of all measured reaction rates in instrumented assemblies. For the same set of fuel assemblies, predicted reaction rates are normalized to the average of all predicted reaction rates. The normalized measured and predicted reaction rates are then accumulated for all maps for the calculation of difference statistics.

3.5.4 2D Reaction Rate Comparisons (movable and fixed in-core detector systems)

For both movable and fixed in-core detector systems, axially integrated reaction rates are used to develop uncertainty factors for 2D quantities FΔH and Fr. For comparisons where both the measured and predicted normalized integral reactions rates are less than 1.0, the differences are discarded because they represent fuel assemblies with less than core average relative power. Low power assemblies not only have higher measurement uncertainty, but they are also not of interest for the determination of peaking factor uncertainty factors because limiting peaking factors are found in high power assemblies.

3.5.5 3D Reaction Rate Comparisons (movable in-core detector systems)

Movable in-core detector systems typically take data at a sufficient number of axial locations to represent well a 3D quantity such as FQ. The detailed measured axial reaction rates are collapsed to the same nodalization as the CMS5 model. Normalized measured and predicted reaction rates at these axial locations are accumulated for all maps for the calculation of difference statistics. As with the 2D reaction rate comparison, if both the measured and predicted nodal reaction rates are less than 1.0, then they are discarded.

3.5.6 3D Reaction Rate Comparisons (fixed in-core detector systems)

Fixed in-core detector systems typically have a small number of axial detectors (4-6) that integrate signals over relatively large portions of the axial core height. For these detectors the SIMULATE5 nodal reaction rates are integrated over the corresponding detector elevations and the normalized measured and predicted reaction rates are computed in the same way that they are for the movable in-core detector systems. In this case however the coarse 3D reaction rate comparisons do not exactly estimate the total uncertainty corresponding to a true local power factor (FQ).

A way to characterize the discrepancy is to relate it to 3D versus 2D reaction rate statistics. Assuming that the sample sizes for both are large enough such that the tolerance limit mechanics do not skew the results, the 2D uncertainties tend to be smaller than the corresponding 3D uncertainties because the 2D data has been averaged. In the same way, the large area of the fixed in-core detectors tends to average out extreme variations in the signal resulting in smaller uncertainties than the detailed nodal data. From the standpoint of estimating FQ uncertainties this averaging process appears as a bias.

To estimate the size of this bias the following calculation is performed.

1. Start with the detailed *movable* in-core detector data from the benchmark cycles in Section 4.3.7.
2. Compute the 3D reaction rate differences for the detailed nodal data.
3. Collapse the detailed reaction rate data over the 4 detector regions, assuming the same size (and location) as a typical fixed in-core detector system.
4. Compute 3D reaction rate differences for the collapsed nodal data.
5. Construct tolerance limits for both the detailed and collapsed data sets.
6. Take the difference between the detailed and collapsed tolerance limits. This difference is the bias that will be applied directly to fixed in-core 3D reaction rate tolerance limits computed from the flux map data.

When the above exercise is applied to the 3D movable in-core detector reaction rate data described in Section 4.3.7, the following bias is identified:

$$3D\ R.R._{Fixed\ Incore\ Bias} = \{\quad\}$$

The total 3D reaction rate tolerance limit for fixed in-core detectors would then become:

$$3D\ R.R._{Fixed\ Incore\ Lower\ T.L.} = 3D\ R.R._{Lower\ T.L.} + \{\quad\}$$

The $3D\ R.R._{Fixed\ Incore\ Bias}$ component of the fixed in-core 3D tolerance limit has been computed with a large amount of data using specialized tools. For this reason the { } bias value is presented for review and approval and no mechanism is presented to allow licensees to change this bias value within the context of this topical report methodology.

3.5.7 Pin-To-Box Lower Tolerance Limit

There are various ways that the pin-to-box lower tolerance limit can be estimated. A previously reviewed submittal [1] used a direct Simulate-to-MCNP approach to estimate the pin-to-box lower tolerance limit. In this report a two-step process [2] (CASMO5 to measured, SIMULATE5 to CASMO5) is used to estimate the pin-to-box lower tolerance limit component of the peak pin power lower tolerance limit.

The first step is the generation of tolerance limits between CASMO5 and measured pin-by-pin fission rates. The fission rates are a close surrogate to pin powers. The pin-by-pin fission rate comparisons are the same as those discussed in Section 2.3. The fission rate tolerance limits are presented in Figure 3-1 and Table 3-3. The "All thermal UO2" set is the most relevant to the analysis of UO2 PWR lattices, since it excludes MOX experiments as well as the U-238 fast fission data. Since the fission rate measurements are serving as a proxy for the pin powers, the U-235 thermal fission data is the data of interest for application to thermal PWRs.

The larger relative errors observed in Figure 3-1 occur in low–power pins. Although the tolerance limits could be decreased by discriminating out the low power pins using a cutoff value, the different normalization schemes across the various critical experiments make this challenging and therefore no such discrimination is employed here. When constructing an uncertainty factor for peak pin power, the only concern is under predicting the magnitude of the pin power so the negative tolerance limit for "All thermal UO2" is selected for the first component of the pin-to-box lower tolerance limit:

$$CASMO5 - to - Experiment_{Lower\ T.L.} = \{\quad\}$$

The second step is the generation of tolerance limits for the differences between pin-to-box ratios as computed by SIMULATE5 and CASMO5. The comparisons involve a comprehensive range of lattice, enrichment, and burnable poison types. The results of these comparisons are presented in Figure 3-2 and Table 3-4. Again, under prediction is the only concern for peaking factor uncertainty factors so the negative tolerance limit for "All" data is selected for the second component of the pin-to-box lower tolerance limit:

$$SIMULATE5 - to - CASMO5_{Lower\ T.L.} = \{\quad\}$$

The total pin-to-box tolerance limit is the RSS (root sum square) of the individual components, multiplied by -1 to preserve the sense of under prediction:

$$Pin - to - Box_{Lower\ T.L.} = -1 \times \sqrt{(\{\quad\})^2 + (\{\quad\})^2} = \{\quad\}$$

The $Pin - to - Box_{Lower\ T.L.}$ has been computed with a large amount of data using specialized tools. For this reason the { } bias value is presented for review and approval and no mechanism is presented to allow licensees to change this bias value within the context of this topical report methodology.

Figure 3-1: CASMO5 to Experiment (or MCNP) Fission Rate Tolerance Limits

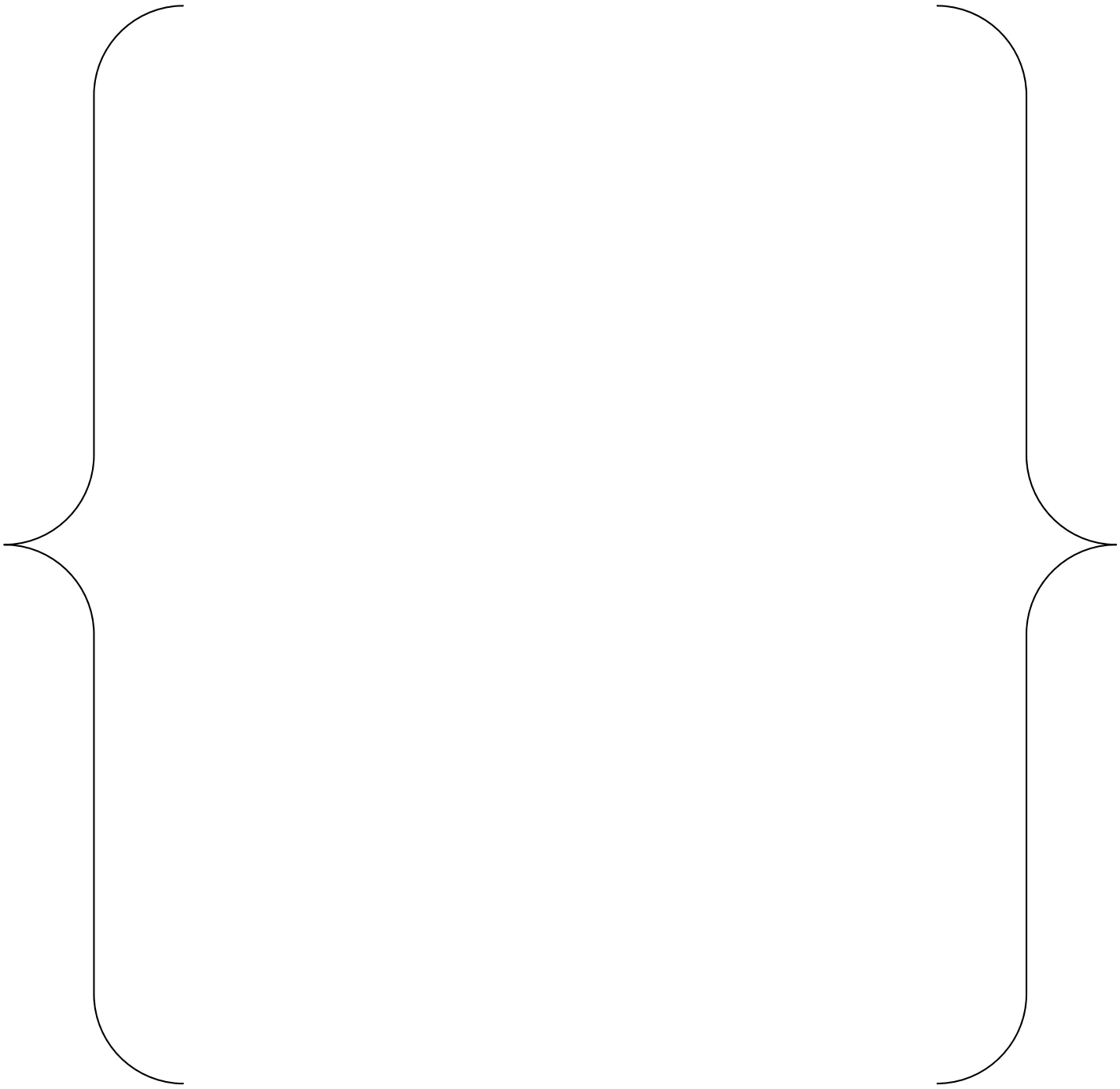

Note: The vertical lines are the 95/95 one-sided tolerance limits.
A value of N denotes the data set is normally distributed.

Table 3-3: CASMO5-to-Experiment fission rate tolerance limits.

Set	Samples	Normal	Lower TL (%)	Upper TL (%)
All thermal UO2	465		{ }	{ }
All UO2	549		{ }	{ }
All	628		{ }	{ }
BW 1810	192		{ }	{ }
BW 1810 core 01	32	*N*	{ }	{ }
BW 1810 core 05	32	*N*	{ }	{ }
BW 1810 core 12	32	*N*	{ }	{ }
BW 1810 core 14	32			
BW 1810 core 18	32	*N*	{ }	{ }
BW 1810 core 20	32			
DIMPLE	186		{ }	{ }
DIMPLE S06A	92		{ }	{ }
DIMPLE S06A U235	51	*N*	{ }	{ }
DIMPLE S06A U238	41			
DIMPLE S06B	94		{ }	{ }
DIMPLE S06B U235	51			
DIMPLE S06B U238	43	*N*	{ }	{ }
IFBA	140		{ }	{ }
IFBA WH15	62	*N*	{ }	{ }
IFBA WH15 016	31	*N*	{ }	{ }
IFBA WH15 148	31	*N*	{ }	{ }
IFBA WH17	78	*N*	{ }	{ }
IFBA WH17 016	39	*N*	{ }	{ }
IFBA WH17 264	39	*N*	{ }	{ }
KRITZ 3	110		{ }	{ }
KRITZ 3 Pu	79		{ }	{ }
KRITZ 3 Pu WH1 hot	22			
KRITZ 3 Pu WH2 cold	29			
KRITZ 3 Pu WH2 hot	28			
KRITZ 3 U	31			
KRITZ 3 U WH1 hot	11	*N*	{ }	{ }
KRITZ 3 U WH2 hot	20			

Note: A value of $\mathcal{N}$ denotes the data set is normally distributed.

Figure 3-2: SIMULATE5-to-CASMO5 Pin Power Tolerance Limits

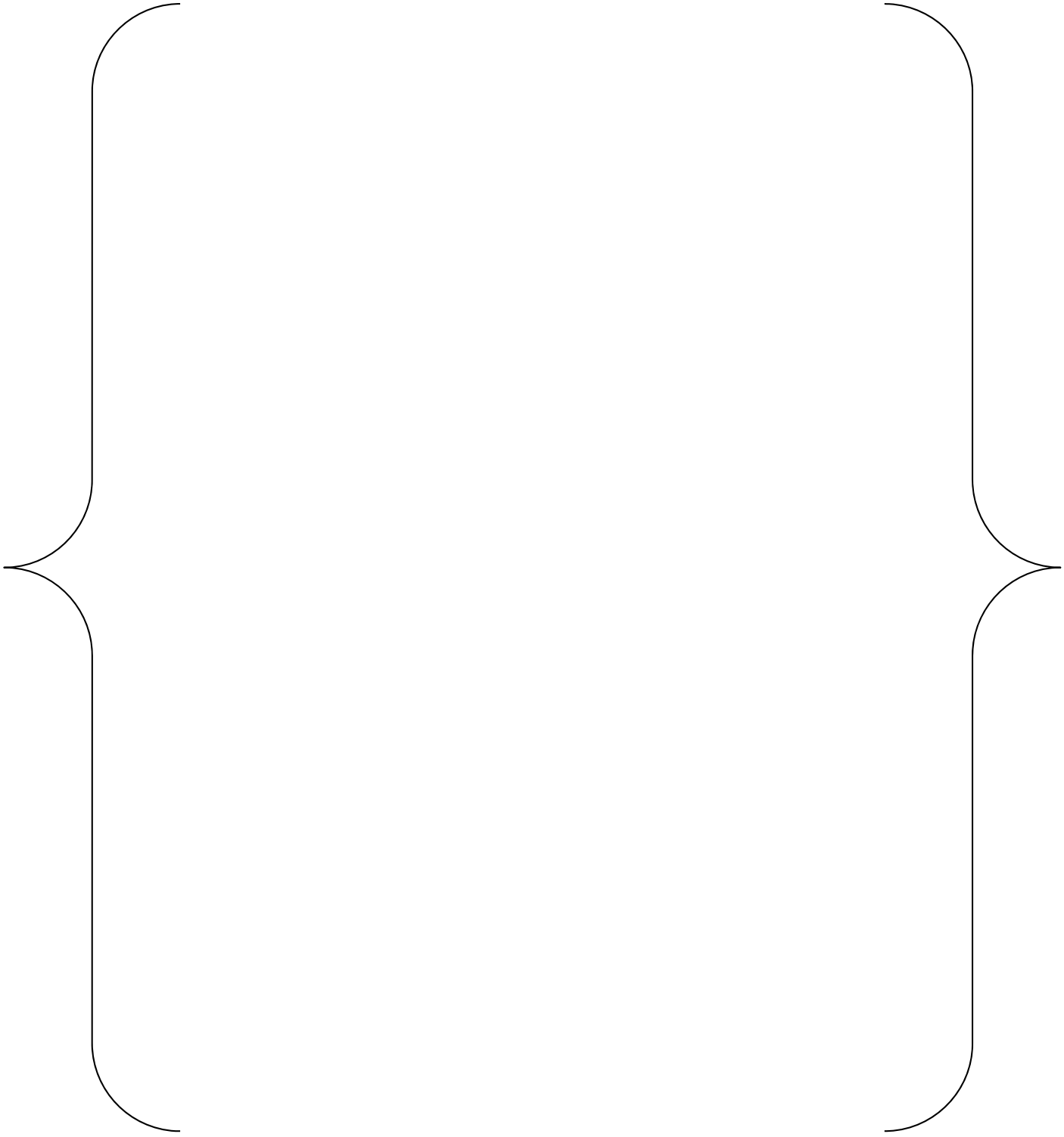

Note: The vertical lines are the 95/95 one-sided tolerance limits.
All data sets are assumed to be non-normal.

Table 3-4: SIMULATE5-to-CASMO5 Pin Power Tolerance limits.

Set	Samples	Lower TL (%)	Upper TL (%)
all	535,248	{ }	{ }
WH14	77,328	{ }	{ }
WH15	117,504	{ }	{ }
WH17	266,112	{ }	{ }
CE14	74,304	{ }	{ }
2.5% enr	178,416	{ }	{ }
3.5% enr	178,416	{ }	{ }
5% enr	178,416	{ }	{ }
10 ppm boron	178,416	{ }	{ }
1250 ppm boron	178,416	{ }	{ }
2500 ppm boron	178,416	{ }	{ }
symmetric gd	134,244	{ }	{ }
asymmetric gd	134,244	{ }	{ }
IFBA	132,516	{ }	{ }
no BPs	134,244	{ }	{ }
no rods	117,936	{ }	{ }
AIC rods	117,936	{ }	{ }
B4C rods	62,784	{ }	{ }
hafnium rods	38,016	{ }	{ }
Pyrex rods	93,168	{ }	{ }
tungsten rods	38,016	{ }	{ }

Note: All data sets are assumed to be non-normal.

3.5.8 FΔH/Fr Total Peaking Factor Uncertainty (movable and fixed in-core detector systems)

The total *FΔH/ Fr* peaking factor tolerance limit (%) is the root sum square (RSS) of the 2D reaction rate lower tolerance limit and the pin-to-box ratio lower tolerance limit (multiplied by -1 to preserve the sense of under prediction):

$$F\Delta H/Fr_{Lower\ T.L.} = -1 \times \sqrt{(2D\ R.R._{Lower\ T.L.})^2 + (\{\quad\})^2}$$

The corresponding nuclear uncertainty factor is:

$$F\Delta H/Fr_{Upper\ NUF} = 1 - \frac{F\Delta H/Fr_{Lower\ T.L.}}{100\%}$$

3.5.9 FQ Total Peaking Factor Uncertainty (movable in-core detector system)

The total *FQ* peaking factor tolerance limit (%) is the root sum square (RSS) of the 3D reaction rate lower tolerance limit and the pin-to-box ratio lower tolerance limit (multiplied by -1 to preserve the sense of under prediction):

$$FQ_{Lower\ T.L.} = -1 \times \sqrt{(3D\ R.R._{Lower\ T.L.})^2 + (\{\quad\})^2}$$

The corresponding nuclear uncertainty factor is:

$$FQ_{Upper\ NUF} = 1 - \frac{FQ_{Lower\ T.L.}}{100\%}$$

3.5.10 FQ Total Peaking Factor Uncertainty (fixed in-core detector system)

The total *FQ* peaking factor tolerance limit (%) is the root sum square (RSS) of the 3D reaction rate lower tolerance limit (including the *FQ* bias described in Section 3.5.6) and the pin-to-box ratio lower tolerance limit (multiplied by -1 to preserve the sense of under prediction):

$$FQ_{Lower\ T.L.} = -1 \times \sqrt{(3D\ R.R._{Lower\ T.L.} + [\{\quad\}])^2 + (\{\quad\})^2}$$

The corresponding nuclear uncertainty factor is:

$$FQ_{Upper\ NUF} = 1 - \frac{FQ_{Lower\ T.L.}}{100\%}$$

3.5.11 References

1. R. A. Hall et al., Dominion, “Qualification of the Studsvik Core Management System Reactor Physics Methods for Application to North Anna and Surry Power Stations”, DOM-NAF-1-Rev 0.0-P-A, NRC Safety Evaluation Date: March 2003, **NRC Accession Number: ML031690108.**
2. J. Hykes, “Tolerance Limits for SIMULATE5’s Pin-to-Box Predictions”, Studsvik Scandpower, SSP-14-P01/026-C, Rev. 0, Waltham MA, 2015.

3.6 NRFs Derived from Engineering / Physical Arguments

3.6.1 Differential Boron Worth

Differential boron worth is a quantity that is often measured at BOC, HZP as part of startup physics testing. This would seem to make it a good candidate for using the one-sided statistical tolerance limit to determine its uncertainty factor. However, Reference [1] presents evidence that the measurement uncertainty dominates the total uncertainty for this parameter which leads to an overestimation of predictive uncertainty. Reference [1] presented evidence that the statistics generated for differential boron worth, even after attempting to correct for reactivity computer bias, appears excessively large compared to critical boron difference data.

Based on the evidence provided in Reference [1], the upper and lower NRFs for differential boron worth predictions are set to:

$$Differential\ Boron\ Worth_{Upper\ NRF} = \{\quad\}$$

$$Differential\ Boron\ Worth_{Lower\ NRF} = \{\quad\}$$

3.6.2 Doppler Temperature / Power Coefficient

The direct determination of a NRF for Doppler feedback remains very difficult. Benchmarking of CASMO5 Doppler Temperature Defects to Monte Carlo methods (Section 2.3.2.1) suggests that there is very little bias contributed from the CASMO5 cross sections ($\{\approx 3\%\}$). In addition, several operational transients modeled in Section 4.4 include undamped xenon oscillations. The degree of axial stability is determined by the relative balance between the axial shifting xenon distribution and the opposing power-driven fuel temperature change.

The good agreement of the measured and predicted axial offset oscillation magnitude in the modeled operational transient demonstrates that the xenon-Doppler balance is well predicted. The Doppler feedback upper and lower NRFs are therefore set to the following, identical to the values cited in Reference [1]:

$$Doppler\ Coefficient_{UpperNRF} = \{\quad\}$$

$$Doppler\ Coefficient_{Lower\ NRF} = \{\quad\}$$

3.6.3 Kinetics Parameters (Delayed Neutron and Prompt Neutron Lifetime)

The kinetics parameter uncertainties are difficult to evaluate directly so sufficiently conservative values are proposed based on historical precedent. The default (and recommended) basic delayed neutron data set available in CASMO5 is the Tuttle set, which is consistent with the set used for CASMO-4 in Reference [1]. The same kinetics parameters (delayed neutron and prompt neutron lifetime) upper and lower NRFs are set to the same values as in Reference [1]:

$$Kinetics\ Parameter_{Upper\ NRF} = \{\quad\}$$

$$Kinetics\ Parameter_{Lower\ NRF} = \{\quad\}$$

3.6.4 References

1. R. A. Hall et al., Dominion, “Qualification of the Studsvik Core Management System Reactor Physics Methods for Application to North Anna and Surry Power Stations”, DOM-NAF-1-Rev 0.0-P-A, NRC Safety Evaluation Date: March 2003, **NRC Accession Number: ML031690108**

3.7 Change Management

The CMS5 software is, by its nature, changeable. At a minimum, new versions of the software will be issued to correct software errors, but new versions may also be released to add new features or functionality. In addition, recommended modeling practices and biases applied to the code predictions may change over time. Licensees shall implement a graded approach to change management to ensure that any Nuclear Reliability Factors that have been generated remain conservative. The graded approach ranges from normal validation software quality assurance practices for small changes unlikely to impact NRFs all the way to a complete regeneration of NUFs for major software and model changes.

3.8 Conclusion

A rigorous one-sided tolerance limit statistical analysis methodology has been presented that allows licensees to generate tolerance limits, NUFs, and NRFs for most physics parameters important to core design and safety analysis. For those parameters that do not use the statistical analysis method, NRFs have been presented for specific review and approval, as well as for certain elements of the peaking factor methodology cited in the text. For these values, no mechanism is presented to allow licensees to alter them within the context of this topical report methodology.

The next major section, Section 4, uses an extensive amount of plant measured data to both demonstrate the construction of NUFs using the methodology presented above and to present NRFs that are generically applicable to most PWR applications.

4. CMS Benchmark, NUF Methodology Demonstration, and Development of Generically Applicable NRFs

4.1 Introduction

In this section of the report, 63 cycles of measured plant data is used for the following three purposes:

4.1.1 Benchmark

The first use of this plant data is as a traditional integrated benchmark of the CMS5 code system. To model plant operational data, CASMO5 cross sections are generated and passed to the SIMULATE5 core models. This integrated benchmark tests many of the calculations that can be performed by the CMS5 system:

1. Core Reactivity (soluble boron concentration / boron worth)
2. Flux and Power distributions (radial, axial, local peaking)
3. Fuel burnup
4. Fuel and burnable poison nuclide concentrations as a function of fuel burnup
5. Integral and differential control rod bank worths
6. Moderator and Doppler temperature coefficients and defects
7. Operational transient simulation
8. Generation of delayed neutron parameters and prompt neutron lifetime
9. Detector reaction rates, coupling coefficients, and peaking factors for flux map analysis
10. Fixed source neutron multiplication
11. Ex-core detector response

Most of these code capabilities are demonstrated (explicitly or implicitly) by generating predicted versus measured difference data for various physics parameters. In addition, several operational transients are modeled to demonstrate Doppler/xenon response, fixed source neutron multiplication /ex-core detector response, and overall code fidelity.

4.1.2 Nuclear Uncertainty Factor Methodology Demonstration

The second use of the 63 cycle measured plant data is to provide a worked example of the uncertainty factor methodology (specifically the one-sided tolerance limit statistical analysis) described in Section 3 of this report. NUFs are created from the difference data generated for the benchmark for the physics parameters described in Section 3.

4.1.3 Generically Applicable Nuclear Reliability Factors

Finally, sufficiently conservative PWR NRFs are proposed based upon the NUFs generated so that licensees ***may*** use them without deriving their own NUFs **if** their nuclear units and particular application are within the bounds described in Section 3.1.3.

4.2 Description of Measured Benchmark Data

The 63 cycles of benchmark data are from seven PWR units located at four plant sites. These cycles include various pin lattice and fuel vendor designs and represent evolutionary changes in fuel enrichment, fuel density, fuel loading pattern strategy, spacer grid design and material, core operating conditions, and burnable poison material and design.

The five plants benchmarked in this report have been given generic designations “A” through “E”. Table 4-1 provides a description of the five plants which include different NSSS designs, number of assemblies, fuel lattice designs, and power distribution measurement systems.

Table 4-2 through Table 4-8 list details of each cycle that has been benchmarked, including thermal power rating, fuel enrichments, burnable absorbers (or “poisons”) used, and cycle fuel exposures achieved. The burnable absorber types used in the benchmark cycles are:

1. **B4C** –Discrete BP rods placed in the assembly guide tubes. Contains B_4C-Al_2O_3 pellets, axially zoned and in various radial configurations from 2 pins to 24 pins, including various asymmetric arrangements.
2. **WABA** – Wet Annular Burnable Absorber (WABA) discrete BP rods placed in the assembly guide tubes. Contains B_4C-Al_2O_3 annular pellets with an inner and outer Zircaloy clad and moderator in the center.
3. **Gadolinia** – 2 to 8 w/o Gd_2O_3 mixed with UO_2 as part of the fuel pellets.
4. **IFBA** - Integral Fuel Burnable Absorber (IFBA), ZrB_2 coating applied to UO_2 pellets.

Table 4-1: Benchmark Plant Description

Generic Designation	PWR NSSS	Number of coolant loops	In-core Detector Type	Number of Assemblies	Pin Lattice
"A"	W	2	Movable	121	14x14 (offset instrument tube)
"B"	C.E.	2	Fixed	217	14x14 (large water holes)
"C"	W	4	Movable	193	17x17
"D"	W	3	Movable	157	17x17
"E"	W	3	Movable	157	15x15

**Table 4-2: Plant "A" (Westinghouse 2-Loop)
Benchmark Cycle Details
(7 Cycles)**

Cycle	Thermal Rating (MWt)	Absorber Type	Reload Pellet Enrichment Range	End of Cycle Burnup (GWD/MTU)
A1C26	1650/1772	Gadolinia	2.60-4.95	17400
A1C27	1772	Gadolinia	2.60-4.92	16977
A1C28	1772	Gadolinia	2.60-4.95	17856
A1C29	1772	IFBA	2.60-4.40	18460
A1C30	1772	IFBA	2.60-4.90	18124
A1C31	1772	IFBA	2.60-3.70	13837
A1C32	1772	IFBA	2.60-4.90	13325

**Table 4-3: Plant "B" (Combustion Engineering 2-Loop)
Benchmark Cycle Details
(10 Cycles)**

Cycle	Thermal Rating (MWt)	Absorber Type	Reload Pellet Enrichment Range	End of Cycle Burnup (GWD/MTU)
B2C14	2700	Gadolinia	0.72-4.30	19062
B2C15	2700	Gadolinia	2.15-4.43	16105
B2C16	2700	Gadolinia	2.20-4.40	15182
B2C17	2700	Gadolinia	2.15-4.30	15383
B2C18	2700	Gadolinia	2.25-4.50	15649
B2C19	2700	Gadolinia	2.25-4.50	14796
B2C20	2700	Gadolinia	2.20-4.30	15182
B2C21	2700	Gadolinia	2.20-4.25	15201
B2C22	2700	Gadolinia	2.20-4.35	15336
B2C23	2700	Gadolinia	2.20-4.35	15428

**Table 4-4: Plant "C" (Westinghouse 4-Loop)
Benchmark Cycle Details
(6 Cycles)**

Cycle	Thermal Rating (MWt)	Absorber Type	Reload Pellet Enrichment Range	End of Cycle Burnup (GWD/MTU)
C3C11	3411	IFBA	2.60-4.95	20017
C3C12	3411	IFBA	2.60-4.95	19770
C3C13	3650	IFBA	2.60-4.90	20041
C3C14	3650	IFBA	2.60-4.95	20845
C3C15	3650	IFBA	2.60-4.95	20970
C3C16	3650	IFBA	2.60-4.95	20536

Table 4-5: Plant "D" Unit 1 (Westinghouse 3-Loop) Benchmark Cycle Details (10 Cycles)

Cycle	Thermal Rating (MWt)	Absorber Type	Reload Pellet Enrichment Range	End of Cycle Burnup (GWD/MTU)
D1C15	2893	B4C	4.15-4.25	20021
D1C16	2893	B4C	4.25-4.40	19829
D1C17	2893	B4C	4.45-4.55	19815
D1C18	2893	B4C	4.25-4.55	20503
D1C19	2893	B4C	4.50-4.55	20416
D1C20	2893	B4C	4.45-4.55	20057
D1C21	2893/2940	B4C	4.40-4.55	20343
D1C22	2940	B4C	4.55	16420
D1C23	2940	IFBA/WABA	3.65-4.40	19812
D1C24	2940	IFBA	4.55	20027

Table 4-6: Plant "D" Unit 2 (Westinghouse 3-Loop) Benchmark Cycle Details (10 Cycles)

Cycle	Thermal Rating (MWt)	Absorber Type	Reload Pellet Enrichment Range	End of Cycle Burnup (GWD/MTU)
D2C14	2893	B4C	4.15-4.25	19809
D2C15	2893	B4C	4.15-4.25	18333
D2C16	2893	B4C	4.30-4.45	17866
D2C17	2893	B4C	4.25-4.40	19156
D2C18	2893	B4C	4.20-4.40	19705
D2C19	2893	B4C	4.50-4.55	19012
D2C20	2893	B4C	4.25-4.50	19249
D2C21	2940	B4C	4.25-4.45	17891
D2C22	2940	B4C	4.25-4.45	19454
D2C23	2940	IFBA/WABA	3.80-4.45	18757

Table 4-7: Plant "E" Unit 1 (Westinghouse 3-Loop) Benchmark Cycle Details (10 Cycles)

Cycle	Thermal Rating (MWt)	Absorber Type	Reload Pellet Enrichment Range	End of Cycle Burnup (GWD/MTU)
E1C16	2546	B4C	4.10-4.25	17544
E1C17	2546	B4C	4.10-4.25	18072
E1C18	2546	B4C	4.10-4.25	16783
E1C19	2546	B4C	4.10-4.25	17004
E1C20	2546	B4C	3.80-4.10	17092
E1C21	2546	B4C/IFBA	3.80-4.25	17709
E1C22	2546	IFBA	3.60-4.25	17398
E1C23	2546	IFBA	3.90-4.25	18518
E1C24	2587	IFBA	3.65-4.10	18348
E1C25	2587	IFBA	3.75-4.00	17868

Table 4-8: Plant "E" Unit 2 (Westinghouse 3-Loop) Benchmark Cycle Details (10 Cycles)

Cycle	Thermal Rating (MWt)	Absorber Type	Reload Pellet Enrichment Range	End of Cycle Burnup (GWD/MTU)
E2C16	2546	B4C	3.80-4.25	16649
E2C17	2546	B4C	4.10-4.25	16877
E2C18	2546	B4C	4.10-4.25	17735
E2C19	2546	B4C	4.10-4.25	17482
E2C20	2546	B4C	4.10-4.25	17540
E2C21	2546	B4C/IFBA	3.70-4.25	18296
E2C22	2546	IFBA	3.65-4.25	18532
E2C23	2546	IFBA	3.65-4.10	16937
E2C24	2587	IFBA	3.95-4.05	17702
E2C25	2587	IFBA	3.85-4.10	17876

4.3 CMS5 Benchmark – Physics Parameters

4.3.1 Introduction

In this section the results of the 63 cycle benchmark are presented. The physics parameters that are compared include critical boron comparisons (core reactivity), control rod worths (integral and peak differential), isothermal temperature coefficients, and reaction rate comparisons from flux maps taken at various times during cycle life.

4.3.2 General Model Options

The 63 benchmark cycles have been modeled according to the Studsvik Scandpower CMS5 Modeling Guidelines using best-estimate input values where possible. Key approximations that were made include using nominal fuel enrichments and average fuel assembly loadings. During the first iteration of comparisons a small ({ } pcm) bias was observed between BOC HZP predictions and measurements. A model bias of { } pcm was applied at HZP and this bias has been made the default value for CMS5 PWR eigenvalue searches at low power.

The SIMULATE5 models in this report have the following options active:

1. Full core radial model
2. 32 axial nodes
3. Radial Sub-mesh option
4. Four energy groups

4.3.3 Core Reactivity (Critical Boron Concentration)

To assess the capability of CMS5 to model core reactivity, predicted critical boron concentrations were compared against plant measurements. B^{10} depletion was taken into account by using data taken at points in cycle life when the B^{10}/B ratio was known, from data at EOL (< 50 ppm) when B^{10} depletion is not significant due to the low boron concentration, or by using a B^{10} correction model. Differences are expressed in terms of reactivity by converting the ppm differences to pcm differences using predicted boron worth.

Table 4-9 presents the results of the core reactivity benchmark. The HZP results are reported as well as the HFP results for various times in cycle life.

Table 4-9: Core Reactivity (Critical Boron) Benchmark Results

Plant	Type	Mean Difference (pcm)	Standard Deviation (pcm)	Number of Observations	Minimum (pcm)	Maximum (pcm)
"A"	BOC, HZP	49	73	7	-75	138
	BOC, HFP	65	57	40	-30	152
	MOC, HFP	69	59	174	-65	183
	EOC, HFP	22	20	21	-35	41
	ALL	64	58	242	-75	183
"B"	BOC, HZP	59	89	10	-35	200
	BOC, HFP	42	73	86	-63	254
	MOC, HFP	-5	79	985	-194	240
	EOC, HFP	-11	105	88	-136	201
	ALL	-2	82	1169	-194	254
"C"	BOC, HZP	33	96	6	-126	152
	BOC, HFP	-32	66	50	-189	84
	MOC, HFP	-55	42	382	-207	23
	EOC, HFP	-9	83	26	-95	117
	ALL	-49	51	464	-207	152
"D"	BOC, HZP	61	108	20	-126	331
	BOC, HFP	17	81	150	-198	254
	MOC, HFP	11	58	298	-119	220
	EOC, HFP	-13	71	152	-125	189
	ALL	8	71	620	-198	331
"E"	BOC, HZP	10	93	20	-261	157
	BOC, HFP	51	71	219	-97	219
	MOC, HFP	96	94	308	-161	253
	EOC, HFP	174	58	214	29	293
	ALL	103	93	761	-261	293
Combined	ALL	23	93	3256	-261	331

4.3.4 Integral Control Rod Bank Worth

The 63 cycles of benchmark data include rod bank worths measured by the boron dilution, rod swap, and dynamic rod worth methods. Reactivity computer kinetics corrections were made to the measurements.

Table 4-10 presents the results of the integral control rod bank worth benchmark.

Table 4-10: Integral Control Rod Bank Worth Benchmark Results

Plant	Mean Difference (%)	Standard Deviation (%)	Number of Observations	Minimum (%)	Maximum (%)
"A"	-1.4	4.1	42	-6.8	9.9
"B"	-2.0	4.8	36	-12.8	8.7
"C"	-2.1	3.7	48	-9.4	4.9
"D"	-0.7	3.2	112	-12.8	7.0
"E"	1.0	3.3	102	-6.6	9.5
Combined	-0.6	3.8	340	-12.8	9.9

4.3.5 Peak Differential Control Rod Bank Worth

For the control rods that were measured using the rod swap or dynamic rod worth method, the peak predicted differential control rod bank worth was compared against the peak measured differential control rod bank worth (regardless of where the peak actually occurred in each case). Reactivity computer kinetics corrections were made to the measurements.

Table 4-11 presents the results of the differential control rod bank worth benchmark.

Table 4-11: Peak Differential Rod Bank Worth Benchmark Results

Plant	Mean Difference (%)	Standard Deviation (%)	No. of Obs.	Minimum (%)	Maximum (%)
"A"	1.1	2.9	5	-1.0	6.0
"B"	-4.5	8.7	4	-15.0	2.7
"C"	2.0	4.3	54	-10.7	10.6
"D"	-2.7	5.7	20	-15.6	7.8
"E"	-1.1	6.0	20	-20.7	6.4
Combined	0.2	5.4	103	-20.7	10.6

4.3.6 Isothermal Temperature Coefficient

For all of the 63 benchmark cycles a BOC, HZP ITC measurement was taken as part of startup physics testing. For this benchmark a predicted heatup and cooldown of ≈5°F was averaged and compared against the measured average ITC.

Table 4-12 presents the results of the isothermal temperature coefficient benchmark.

Table 4-12: Isothermal Temperature Coefficient Benchmark Results

Plant	Mean Difference (pcm/°F)	Standard Deviation (pcm/°F)	No. of Obs.	Minimum (pcm/°F)	Maximum (pcm/°F)
"A"	0.20	0.19	7	-0.09	0.46
"B"	0.51	0.42	10	0.11	1.45
"C"	-0.51	0.11	6	-0.66	-0.38
"D"	-0.27	0.22	20	-0.68	0.33
"E"	-0.11	0.41	20	-0.77	0.72
Combined	-0.07	0.44	63	-0.77	1.45

4.3.7 2D/3D Reaction Rate Comparisons

Predicted 2D and 3D reaction rates are compared against the corresponding measured reactions rates taken from flux map surveillances. Four flux maps are analyzed for each benchmark cycle including one power ascension map (≈70%) and HFP BOC, MOC, and EOC maps.

Plants “A”, “C”, “D” and “E” have movable in-core systems and their flux map data is pooled together. The 10 cycles of Plant “B” flux map data are from a fixed in-core detector system and are presented separately.

Consistent with the peaking factor methodology presented in Section 3.5, normalized low power region (<1.0) comparisons have been excluded from the final data sets.

Table 4-13 and Table 4-14 present the results of the 2D reaction rate comparisons for movable and fixed in-core detector systems respectively.

Table 4-15 and Table 4-16 present the results of the 3D reaction rate comparisons for movable and fixed in-core detector systems respectively.

Table 4-13: 2D Reaction Rate Comparisons for Movable in-core Detectors

Plant	Mean Difference (%)	Standard Deviation (%)	No. of Obs.	Minimum (%)	Maximum (%)
"A"	0.07	1.36	804	-4.86	3.92
"C"	-0.20	1.04	966	-4.42	3.97
"D"	-0.09	1.28	2577	-5.03	6.28
"E"	0.05	1.36	2417	-6.03	5.05
Combined	-0.04	1.29	6764	-6.03	6.28

Table 4-14: 2D Reaction Rate Comparisons for Fixed in-core Detectors

Plant	Mean Difference (%)	Standard Deviation (%)	No. of Obs.	Minimum (%)	Maximum (%)
"B"	-0.14	1.45	1159	-4.43	4.92

Table 4-15: 3D Reaction Rate Comparisons for Movable in-core Detectors

Plant	Mean Difference (%)	Standard Deviation (%)	No. of Obs.	Minimum (%)	Maximum (%)
"A"	0.21	2.22	21039	-40.91*	13.45
"C"	-0.11	1.68	26850	-18.22	14.54
"D"	-0.01	2.29	71382	-14.89	10.51
"E"	0.22	2.42	68611	-17.89	9.78
Combined	0.09	2.26	187882	-40.91	14.54

*Note: Large differences were observed for several end nodes in the Plant "A" dataset. If these values were removed from the dataset the minimum observed value would be consistent with the other plants.

Table 4-16: 3D Reaction Rate Comparisons for Fixed In-core Detectors

Plant	Mean Difference (%)	Standard Deviation (%)	No. of Obs.	Minimum (%)	Maximum (%)
"B"	-0.17	2.16	4498	-12.26	13.66

4.4 CMS5 Benchmark – Plant Transients

4.4.1 Introduction

In this section three normal operation plant transient models are presented as well as a demonstration of the CMS5 sub-critical fixed source solver and ex-core detector models.

Normal operation transients, especially those involving power changes, are useful for demonstrating the ability of the CMS5 model to accurately predict core behavior involving combinations of large power changes, control rod movements, temperature variations, xenon concentration and distribution changes, and boron concentration changes. Included in the following section are brief descriptions of three actual normal operation events followed by the results of modeling those transients.

The last "transient" is a demonstration of the CMS5 sub-critical fixed source solver model combined with the ex-core detector response model as compared to Monte Carlo results.

4.4.2 Plant "D" Unit 2 Cycle 14 Transient

During this transient Plant "D" Unit 2 power was reduced from HFP equilibrium conditions to approximately 27% power on 10/14/2000. After holding at low power for approximately 10 hours, a ramp to 100% power over about 11 hours was initiated.

Figure 4-1 shows the control rod position and power level versus time for the duration of the transient. Figure 4-2 compares the measured (as recorded by ex-core nuclear instrumentation) delta-I and CMS5 predicted delta-I versus time, with delta-I being defined as axial offset multiplied by core percent power. Figure 4-3 compares the measured and CMS5 predicted reactivity in the form of critical boron concentration versus time.

A full-power undamped xenon oscillation begins at about 40 hours (see Figure 4-2). The measured delta-I indicates stable or slightly damped natural axial core behavior. SIMULATE5 demonstrates excellent agreement with the timing and magnitude of the axial oscillation.

SIMULATE5 critical boron values follow the trend in measured values very closely, with a bias of about 45 ppm. This bias is likely attributable largely to a high degree of B^{10} depletion, which has not been accounted for in this transient.

Figure 4-1: Plant "D", Unit 2 Cycle 14 Transient
Control Rod Bank D Position and Power vs. Time

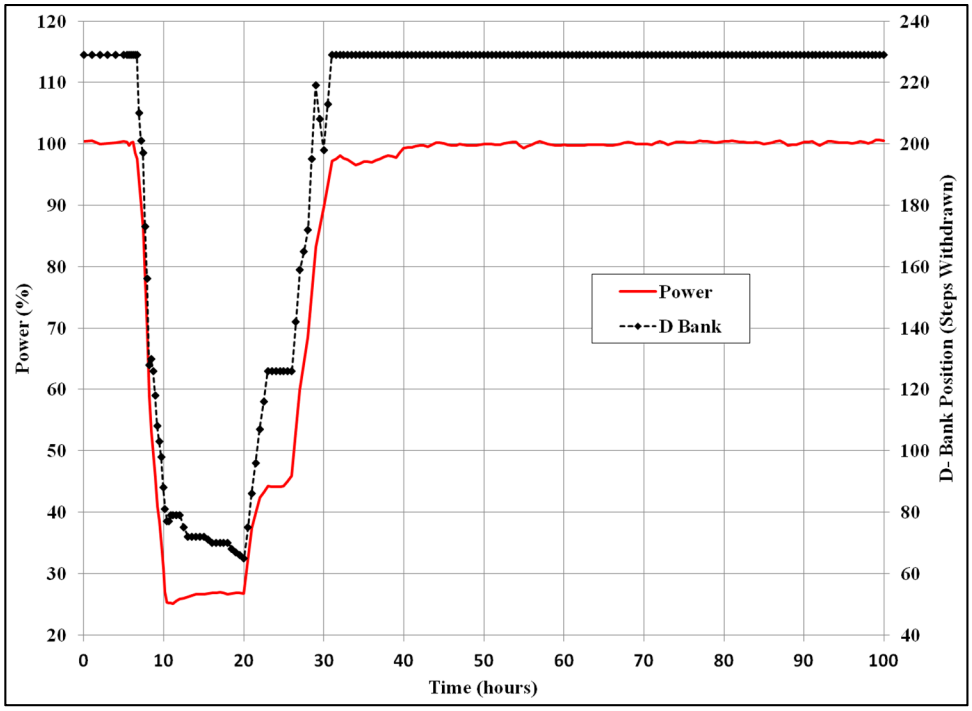

Figure 4-2: Plant "D", Unit 2 Cycle 14 Transient
Delta-I Comparison

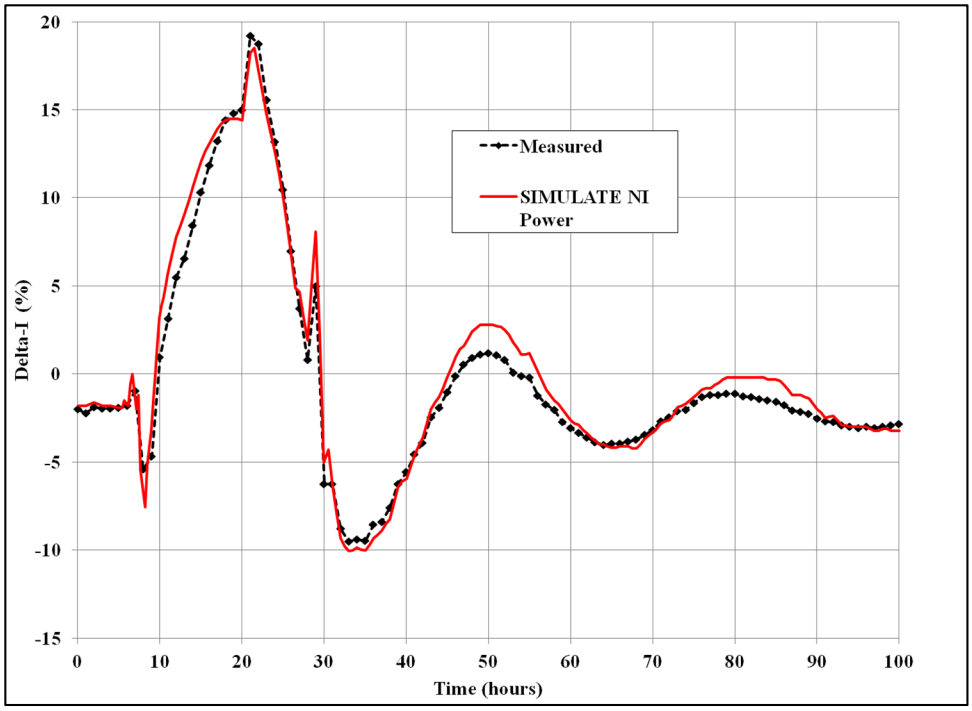

Figure 4-3: Plant "D", Unit 2 Cycle 14 Transient

Reactivity (critical boron) Comparison

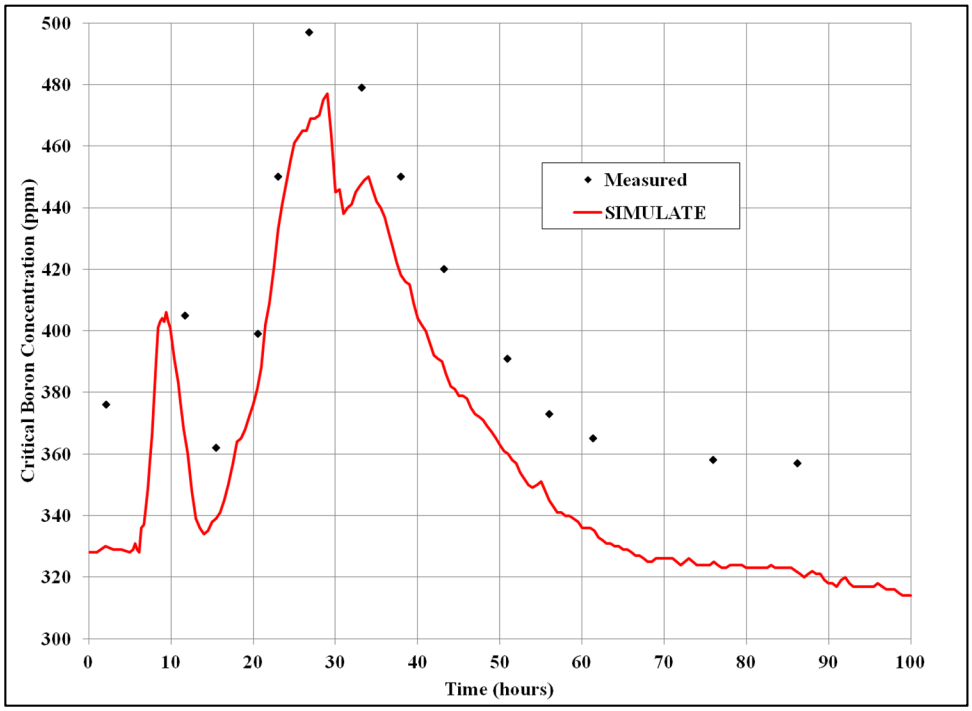

4.4.3 Plant "B" Unit 2 Cycle 23 Transient

On October 2, 2015 Unit 2 of Plant "B" underwent a shutdown using only boron (control rods remained in the all rods out position for the duration of the shutdown).

Figure 4-4 shows the control rod position and power level versus time for the duration of the transient. Figure 4-5 compares the measured Axial Shape Index (ASI) and CMS5 predicted ASI versus time. Figure 4-6 compares the measured and CMS5 predicted reactivity in the form of critical boron concentration versus time.

From Figure 4-5 the predicted axial power agrees very well with the measured. Although there are a sparse number of boron measurements at the beginning of the transient, the predicted critical borons are within 10 ppm of the available measured points.

**Figure 4-4: Plant "B", Unit 2 Cycle 23 Transient
Control Rod Bank 1 Position and Power vs. Time**

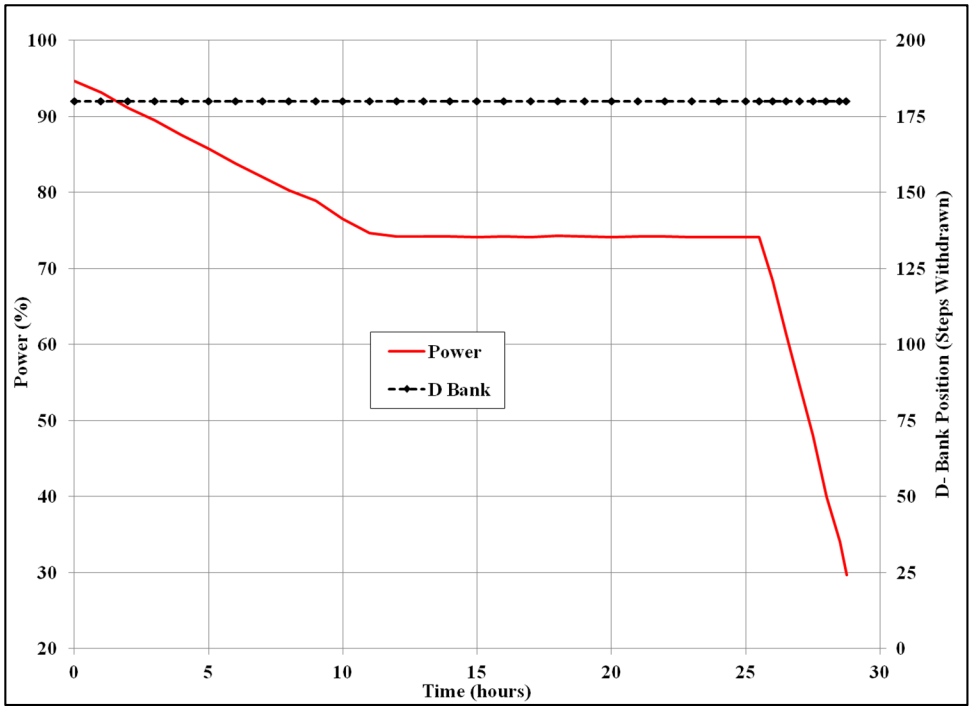

**Figure 4-5: Plant "B", Unit 2 Cycle 23 Transient
ASI Comparison**

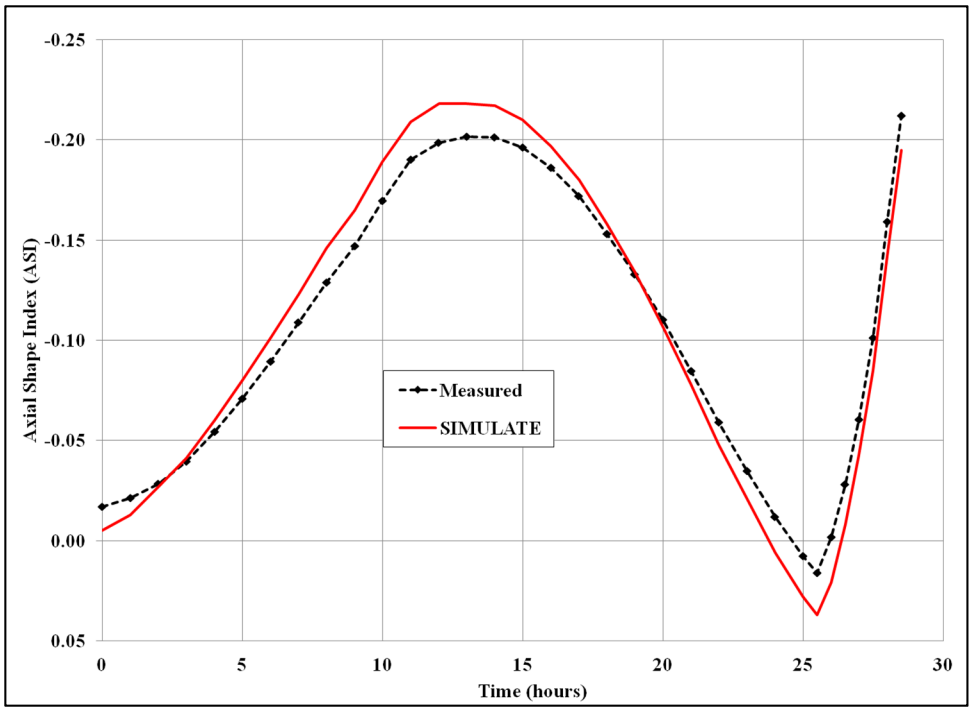

Figure 4-6: Plant "B", Unit 2 Cycle 23 Transient Reactivity (critical boron) Comparison

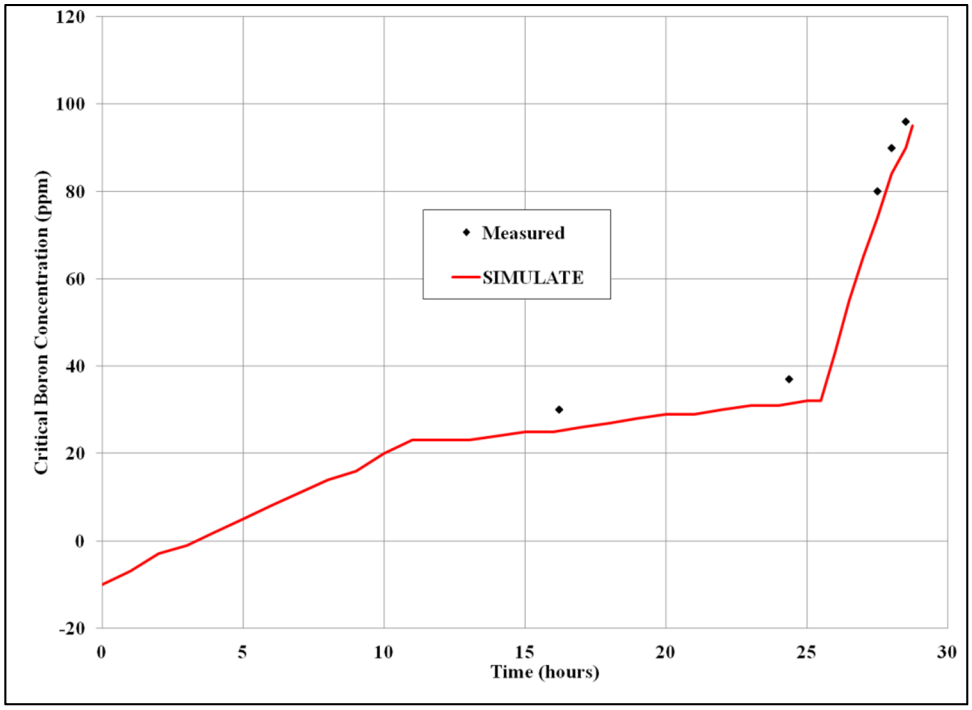

4.4.4 Plant "A" Cycle 27 Transient

Plant "A" power was reduced from HFP equilibrium conditions to approximately 40% power on 2/10/2006. After holding at low power for approximately 65 hours, a ramp to 100% power over about 12 hours was initiated.

Figure 4-7 shows the control rod position and power level versus time for the duration of the transient. Figure 4-8 compares the measured delta-I and CMS5 predicted delta-I versus time. Figure 4-9 compares the measured and CMS5 predicted reactivity in the form of critical boron concentration versus time.

The CMS5 delta-I agrees within 2% of measurements during the entire transient and the reactivity (predicted - measured critical boron) agrees within 32 ppm.

Figure 4-7: Plant "A" Cycle 27 Transient
Control Rod Bank D Position and Power vs. Time

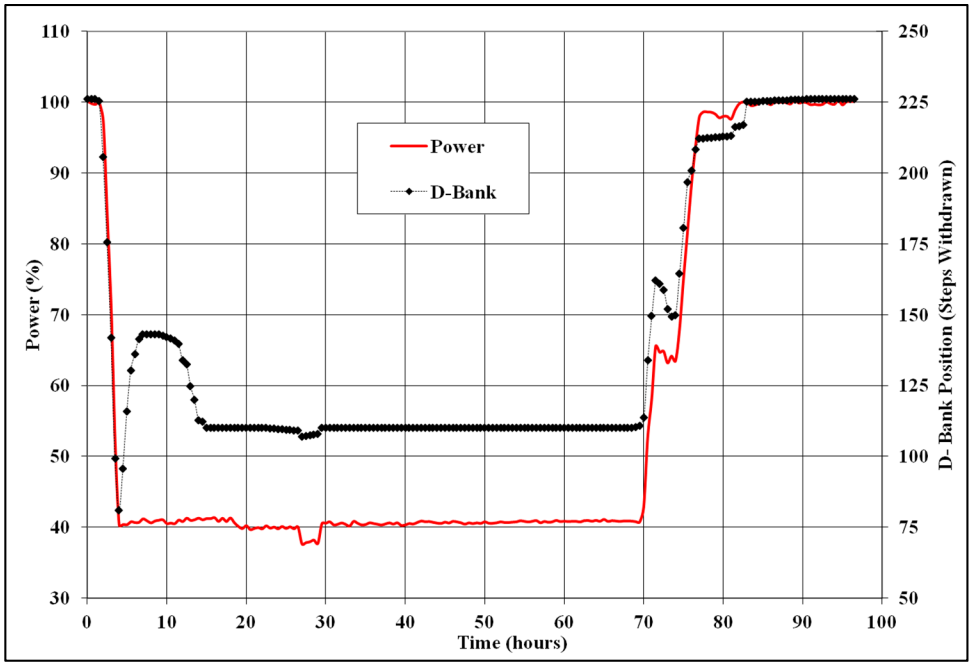

Figure 4-8: Plant "A" Cycle 27 Transient
Delta-I Comparison

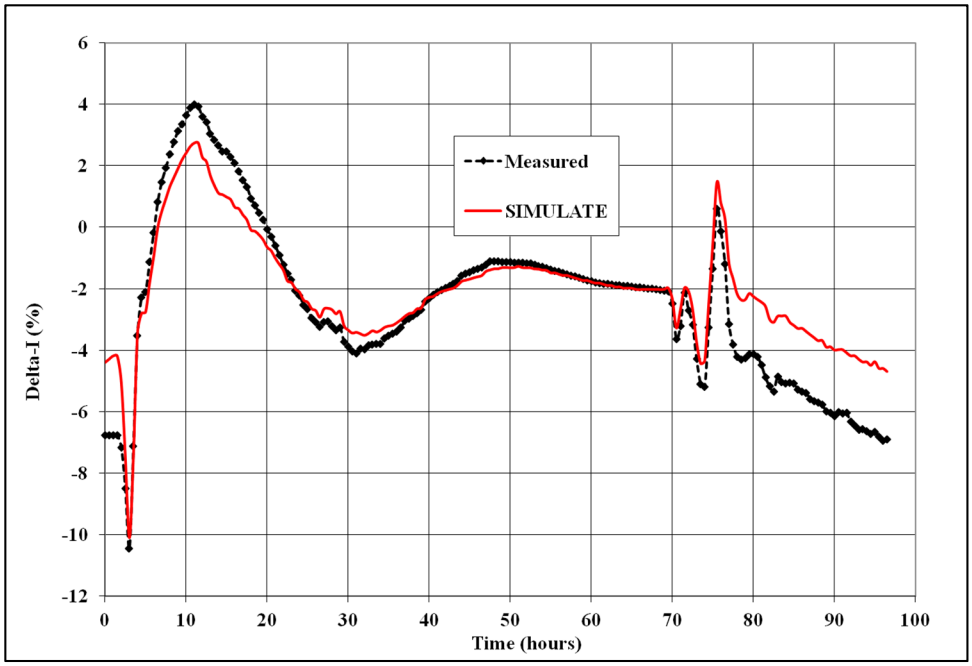

Figure 4-9: Plant "A" Cycle 27 Transient Reactivity (critical boron) Comparison

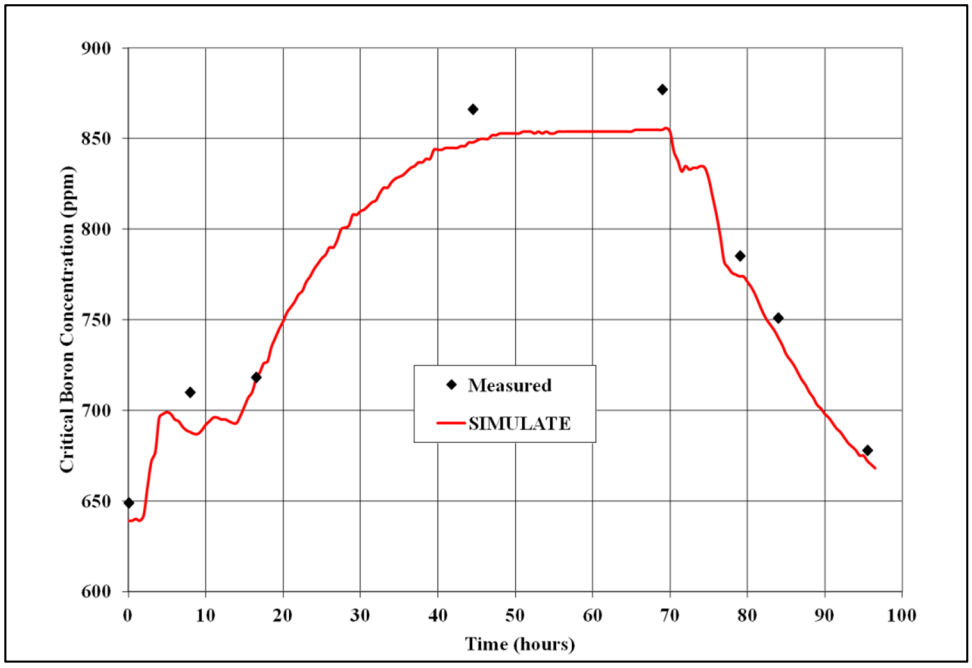

4.4.5 Fixed Source and Ex-core Detector Model Demonstration

CMS5 has the capability to calculate a fixed source solution (in a sub-critical core) taking into consideration both the internal neutron sources from burned fuel (spontaneous fissions and (alpha ,n) sources) as well as from external sources such as secondary source rods. In addition CMS5 has a PWR ex-core detector response model.

In this benchmark the two models are combined to model a hypothetical transient (a boron dilution scenario) in which k-eff increases from far sub-critical (k-eff=0.91) to just before k-eff=1.0. The Inverse Count Rate Ratio (ICRR) for each k-eff is calculated as the ex-core detector response (neutron /$cm^2 \cdot s$) for that state point divided into the beginning detector response, similar to constructing a "1/m" plot during reactor startup.

For this particular scenario a Plant "E", Unit 2, Cycle 26 model at HZP, BOC conditions is used to demonstrate the ex-core detector response for three secondary source arrangements:

1. No secondary source present
2. A secondary source placed two fuel assembly rows away from the ex-core detector
3. A secondary source placed three fuel assembly rows away from the ex-core detector

In each case the CMS5 results are compared against results from a corresponding MCNP6 model. The results of these ICRR calculations are presented in Figure 4-10. CMS5 does an excellent job of matching the MCNP results and showing the improvement in the ICRR curve that is achieved by introducing a secondary source in either row two or three.

Figure 4-10: Fixed Source / Ex-core Detector Benchmark

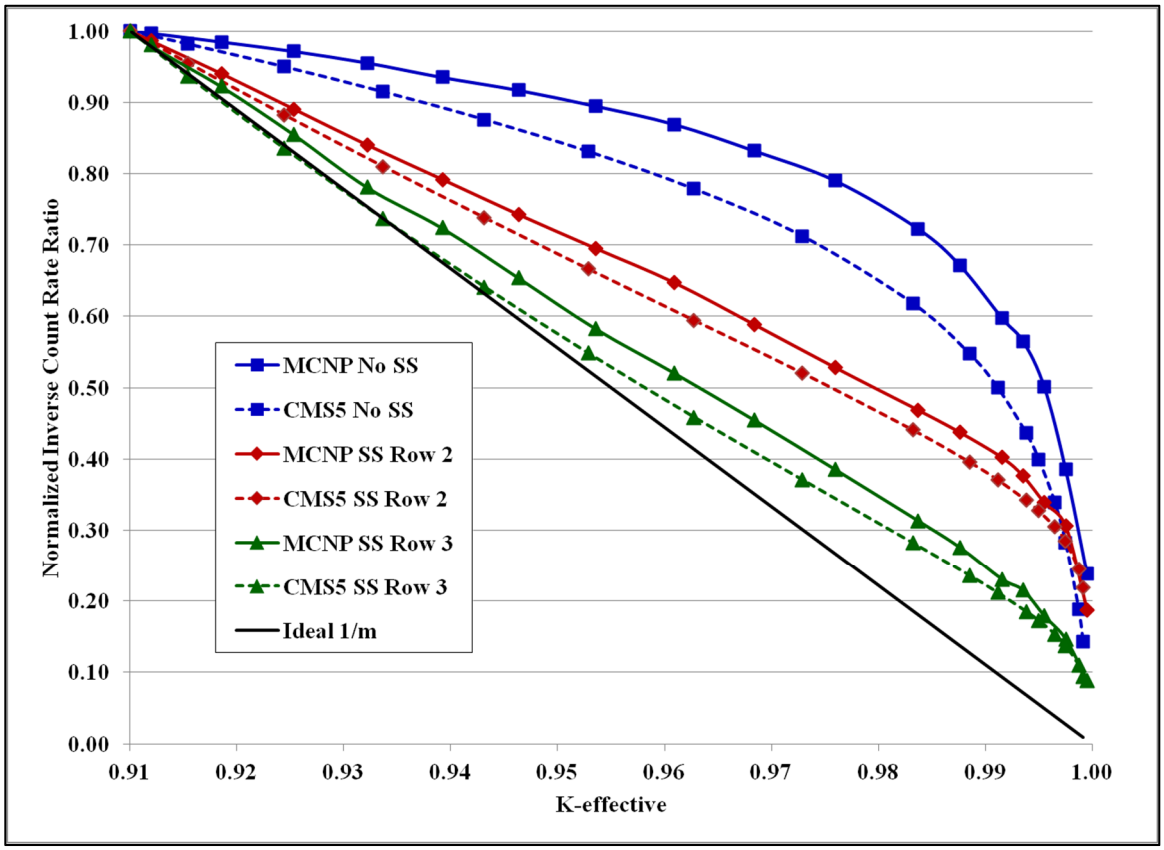

4.5 Nuclear Uncertainty Factor Generation

4.5.1 Introduction

In this section the NUF methodology presented in Section 3 is demonstrated using the 63 cycle benchmark data. For each physics parameter the difference data set characterized in Section 4.3 is tested for normality and then tolerance limits and NUFs are constructed using the appropriate technique.

4.5.2 Core Reactivity NUF

The individual plant and combined core reactivity data sets summarized in Table 4-9 were tested for normality, none of the data sets passed and so each data set was sorted. Based on the number of observations, the appropriate m^{th} value was selected to set the tolerance limits. The upper and lower NUF was determined for the combined data set, and these results are summarized in Table 4-17.

Table 4-17: Core Reactivity Tolerance Limits and NUFs

Plant	No. of Obs.	Dataset Normal?	Non-parametric m^{th} Value	Upper Tolerance Limit (pcm)	Lower Tolerance Limit (pcm)	Upper NUF Value (pcm)	Lower NUF Value (pcm)
"A"	242	No	7	{ }	{ }	-	-
"B"	1169	No	46	{ }	{ }	-	-
"C"	464	No	16	{ }	{ }	-	-
"D"	620	No	22	{ }	{ }	-	-
"E"	761	No	28	{ }	{ }	-	-
Combined	3256	No	143	{ }	{ }	{ }	{ }

4.5.3 Integral Control Rod Bank Worth (Individual and Total Bank Worths) NUF

The individual plant and combined integral rod bank worth data sets summarized in Table 4-10 were tested for normality. All of the data sets passed the normality test so an appropriate K multiplier value was calculated and then combined with the mean and standard deviation to determine the tolerance limits.

For example, for the combined integral control rod bank worth data set, the mean and standard deviation are { } and { } respectively, the K value is 1.79 for 340 observations, so the upper and lower tolerance limits are:

$$TL_L = \overline{X} - (K \times s) = \{\quad\} - (1.79 \times \{\quad\}) = \{\quad\}$$

$$TL_U = \overline{X} + (K \times s) = \{\quad\} + (1.79 \times \{\quad\}) = \{\quad\}$$

The upper and lower NUFs were determined for the combined data set, and these results are summarized in Table 4-18. These values represent the individual control rod bank worths. The total bank worth NUFs are inherently bounded by the individual bank values.

Table 4-18: Integral Control Rod Bank Worth Tolerance Limits and NUFs

Plant	No. of Obs.	Dataset Normal?	K Multiplier	Upper Tolerance Limit (%)	Lower Tolerance Limit (%)	Upper NUF Value	Lower NUF Value
"A"	42	Yes	2.11	{ }	{ }	-	-
"B"	36	Yes	2.16	{ }	{ }	-	-
"C"	48	Yes	2.08	{ }	{ }	-	-
"D"	112	Yes	1.91	{ }	{ }	-	-
"E"	102	Yes	1.92	{ }	{ }	-	-
Combined	340	Yes	1.79	{ }	{ }	{ }	{ }

4.5.4 Peak Differential Control Rod Bank Worth NUF

The individual plant and combined peak differential control rod bank worth data sets summarized in Table 4-11 were tested for normality. Most individual datasets tested as normal, however Plant "E" and the combined data set did not. The appropriate m^{th} value or K multiplier is used to determine the tolerance limits.

The upper and lower NUFs were determined for the combined data set and, these results are summarized in Table 4-19.

Table 4-19: Peak Differential Control Rod Bank Worth Tolerance Limits and NUFs

Plant	No. of Obs.	Dataset Normal?	Non-parametric m^{th} Value	K Multiplier	Upper Tolerance Limit (%)	Lower Tolerance Limit (%)	Upper NUF Value	Lower NUF Value
"A"	5	Yes	-	4.20	{ }	{ }	-	-
"B"	4	Yes	-	5.14	{ }	{ }	-	-
"C"	54	Yes	-	2.05	{ }	{ }	-	-
"D"	20	Yes	-	2.40	{ }	{ }	-	-
"E"*	20	No	N/A	-	N/A	N/A	-	-
Combined	103	No	2	-	{ }	{ }	{ }	{ }

*Note: no individual tolerance limits are listed for the peak differential rod worth for Plant "E" as it is a non-normal data set with less than 60 observations, and therefore a non-parametric m^{th} value cannot be determined.

4.5.5 Isothermal and Moderator Temperature Coefficient NUF

The individual plant and combined isothermal temperature coefficient data sets summarized in Table 4-12 were tested for normality. All of the data sets passed the normality test so an appropriate K multiplier value was calculated and then combined with the mean and standard deviation to determine the tolerance limits.

The upper and lower NUFs were determined for the combined data set, and these results are summarized in Table 4-20.

Table 4-20: Isothermal and Moderator Temperature Coefficient Tolerance Limits and NUFs

Plant	No. of Obs.	Dataset Normal?	K Multiplier	Upper Tolerance Limit (pcm/°F)	Lower Tolerance Limit (pcm/°F)	Upper NUF Value (pcm/°F)	Lower NUF Value (pcm/°F)
"A"	7	Yes	3.40	{ }	{ }	-	-
"B"	10	Yes	2.91	{ }	{ }	-	-
"C"	6	Yes	3.71	{ }	{ }	-	-
"D"	20	Yes	2.40	{ }	{ }	-	-
"E"	20	Yes	2.40	{ }	{ }	-	-
Combined	63	Yes	2.01	{ }	{ }	{ }	{ }

4.5.6 FΔH/Fr Movable In-core Detector NUF

The first step in determining the *FΔH/Fr* NUF is to determine the 2D integral reaction rate lower tolerance limit for the movable in-core detector plants. The individual plant datasets are non-normal and the combined dataset is greater than 5000 observations so non-normality is assumed. The combined dataset non-parametric m^{th} value based on 6764 observations is 309, and the 309^{th} most negative value on the sorted combined list is { }. This is then combined with the pin-to-box lower tolerance limit from Section 3.5.8 to determine the total tolerance limit:

$$F\Delta H/Fr_{Lower\ T.L.} = -1 \times \sqrt{(\{\quad\})^2 + (\{\quad\})^2} = \{\quad\}$$

and the upper NUF (summarized in Table 4-21) is:

$$F\Delta H/Fr_{Upper\ NUF} = 1 - \frac{\frac{F\Delta H}{Fr}_{Lower\ T.L.}}{100\%} = 1 - \frac{\{\quad\}}{100\%} = \{\quad\}$$

Table 4-21: Movable In-core Detector FΔH/Fr Tolerance Limit and NUF

Plant	No. of Obs.	Dataset Normal?	Non-parametric m^{th} Value	Reaction Rate Lower Tolerance Limit (%)	Pin-To-Box Lower Tolerance Limit (%)	Total Lower Tolerance Limit (%)	Upper NUF Value
"A"	804	No	30	{ }	-	-	-
"C"	966	No	37	{ }	-	-	-
"D"	2577	No	111	{ }	-	-	-
"E"	2417	No	103	{ }	-	-	-
Combined	6764	N/A	309	{ }	{ }	{ }	{ }

4.5.7 FΔH/Fr Fixed In-core Detector NUF

The fixed in-core detector *FΔH/Fr* NUF is determined in the same way as the movable detector NUF using the Plant "B" 2D reaction rate statistics. The results of these calculations are summarized in Table 4-22.

Table 4-22: Fixed In-core Detector FΔH/Fr Tolerance Limit and NUF

Plant	No. of Obs.	Dataset Normal?	Non-parametric m^{th} Value	Reaction Rate Lower Tolerance Limit (%)	Pin-To-Box Lower Tolerance Limit (%)	Total Lower Tolerance Limit (%)	Upper NUF Value
"B"	1159	No	46	{ }	{ }	{ }	{ }

4.5.8 FQ Movable In-core Detector NUF

The first step in determining the *FQ* NUF is to determine the 3D nodal reaction rate lower tolerance limit for the movable in-core detector plants. All of the datasets involved had a number of observations outside the range of the Shaprio-Wilk normality test so the data is all treated as non-normal. The combined data set non-parametric m[th] value based on 187882 observations is 9239, and the 9239[th] most negative value on the sorted combined list is { }. This is then combined with the pin-to-box lower tolerance limit from Section 3.5.8 to determine the total tolerance limit:

$$FQ_{Lower\ T.L.} = -1 \times \sqrt{(\{\quad\})^2 + (\{\quad\})^2} = \{\quad\}$$

and the upper NUF (summarized in Table 4-23) is:

$$FQ_{Upper\ NUF} = 1 - \frac{FQ_{Lower\ T.L.}}{100\%} = 1 - \frac{\{\quad\}}{100\%} = \{\quad\}$$

Table 4-23: Movable In-core Detector FQ Tolerance Limit and NUF

Plant	No. of Obs.	Dataset Normal?	Non-parametric m[th] Value	Reaction Rate Lower Tolerance Limit (%)	Pin-To-Box Lower Tolerance Limit (%)	Total Lower Tolerance Limit (%)	Upper NUF Value
"A"	21039	N/A	1000	{ }	-	-	-
"C"	26850	N/A	1284	{ }	-	-	-
"D"	71382	N/A	3474	{ }	-	-	-
"E"	68611	N/A	3337	{ }	-	-	-
Combined	187882	N/A	9239	{ }	{ }	{ }	{ }

4.5.9 FQ Fixed In-core Detector NUF

The fixed in-core detector *FQ* NUF is determined much like the movable NUF, with the addition of the fixed in-core *FQ* bias value (Section 3.5.6) that is added to the Plant "B" reaction rate tolerance limit before being root sum-squared with the pin-to-box lower tolerance limit value. The dataset is not normal and the 201st (based on 4498 observations) most negative 3D reaction rate difference is { }.

$$FQ_{Lower\ T.L.} = -1 \times \sqrt{(\{\quad\} + [\{\quad\}])^2 + (\{\quad\})^2} = \{\quad\}$$

and the upper NUF (summarized in Table 4-24) is:

$$FQ_{Upper\ NUF} = 1 - \frac{FQ_{Lower\ T.L.}}{100\%} = 1 - \frac{\{\quad\}}{100\%} = \{\quad\}$$

Table 4-24: Fixed In-core Detector FQ Tolerance Limit and NUF

Plant	No. of Obs.	Dataset Normal?	Non-parametric m^{th} Value	Reaction Rate Lower Tolerance Limit (%)	Fixed In-core FQ R.R. Bias (%)	Pin-To-Box Lower Tolerance Limit (%)	Total Lower Tolerance Limit (%)	Upper NUF Value
"B"	4498	No	201	{ }	{ }	{ }	{ }	{ }

4.6 Generic Nuclear Reliability Factors

The extensive 63 cycle benchmark includes design and operational data that is representative of nearly all operating PWRs. As such the generic Nuclear Reliability Factors in Table 4-25 are presented for review and approval with the intent that they may be used for in-scope applications by licensees without the need to first exercise the methodology presented in Section 3.

These NRFs are set to convenient values that are more conservative than their corresponding NUFs. This conservatism reduces the risk that small variations in the NUFs (resulting from software/model updates) would cause a change to the NRFs (as long as the NRFs remain bounding).

Table 4-25: Generic Nuclear Reliability Factors

Physics Parameter	NRF	
	Upper	**Lower**
Core Reactivity (Critical Boron Concentration)	{ } pcm	{ } pcm
Integral Control Rod Bank Worth (Individual Bank and Total of All Banks)	{ }	{ }
Peak Differential Control Rod Bank Worth	{ }	{ }
Isothermal and Moderator Temperature Coefficient	{ } pcm/°F	{ } pcm/°F
FΔH / Fr (Movable and Fixed In-core detectors)	{ }	N/A
FQ (Movable and Fixed In-core detectors)	{ }	N/A
Differential Boron Worth	{ }	{ }
Doppler Temperature / Power Coefficient	{ }	{ }
Kinetics Parameters (Delayed Neutron and Prompt Neutron Lifetime)	{ }	{ }

4.7 Conclusion

An extensive 63 cycle benchmark has been performed and excellent agreement between CMS5 predictions and measurements were observed for core reactivity, integral and peak differential control rod bank worth, isothermal temperature coefficient, and 2D/3D reaction rates.

The Nuclear Uncertainty Factor methodology of Section 3 was demonstrated for the benchmark physics parameters. In addition, appropriately conservative generic Nuclear Reliability Factors are proposed for PWR applications within the scope defined in Section 3.1.3.

5. Summary and Conclusions

Studsvik Scandpower has demonstrated the accuracy of CASMO5/SIMULATE5 core models through an extensive set of benchmarks including validation to critical experiments and higher-order codes and a 7 unit / 63 cycle comparison of predictions to PWR plant data.

In addition, a rigorous methodology was presented to calculate Nuclear Uncertainty Factors for physics parameters for which CMS5 predictions can be compared against measurements or higher-order codes.

Finally, based on the extensive nature of the 63 cycle benchmark that includes a wide array of PWR design and operating data, a set of conservative generic Nuclear Reliability Factors were determined to account for model predictive bias and uncertainty.

Studsvik Scandpower concludes that the CASMO5 / SIMULATE5 models, in conjunction with the generic Nuclear Reliability Factors, are fully qualified for use as equivalent replacements for prior models. Furthermore, a robust model development process has been described that, coupled with code and model quality assurance practices, provides assurance that future changes to core designs or software will be modeled with accuracy and appropriate conservatism.